Master's Thesis – Integrated Climate System Sciences

Synergies and conflicts between multiple sustainability goals

Jan Steinhauser

School of Integrated Climate System Sciences

Universität Hamburg

Hamburg, December 9, 2020
Editorially revised January 2021

This thesis has been accepted as a Master's Thesis by the Department Geowissenschaften der Universität Hamburg. This is a contribution to the topic: **"Alternative land-use transformation pathways in Germany – Synergies and conflicts between multiple sustainability goals"**.

1. Reviewer: Prof. Dr. Uwe A. Schneider
Research Unit Sustainability & Global Change
Universität Hamburg
2. Reviewer: Dr. Livia Rasche
Research Unit Sustainability & Global Change
Universität Hamburg

Synergies and conflicts between multiple sustainability goals

by

Jan Steinhauser

Abstract

Humanity has made great strides, reducing poverty, hunger, and childhood mortality. However, alongside these positive developments, environmental damages are also increasing, moving the Earth system steadily towards planetary boundaries and out of its safe operating space, creating new and amplifying existing risks to human welfare. Sustainable development is thus an intricate balance of many different aspects, social and environmental, reflected in the 2015 UN Sustainable Development Goals. One sector at the core of this balance is land use, with agriculture ensuring healthy food for all while also impacting several critical Earth systems at the risk of tipping into irreversible, rapid changes, detrimental to humanity.

To better our understanding of these impacts and the connection between them, and to help shape sustainable pathways within these boundaries, I estimate the interconnection, synergies, and conflicts between different Earth system impacts from the land-use sector, using a partial-equilibrium agricultural sector model. I model production, consumption, and trade of key crop and livestock products in and between 28 countries and 5 rest-of-the-world regions as well as their impacts on climate change, biosphere integrity, biogeochemical flows of nitrogen and phosphorus, freshwater use, and land-system change. In six scenarios, I tax different externalities associated with critical Earth system processes and planetary boundaries to investigate how the modeled sustainability impact indicators change.

The results show strong synergies between reducing greenhouse gas emissions, biodiversity loss, water use, and phosphorus pollution from land-use, with weaker and one-sided synergies regarding synthetic nitrogen application. Interconnections with land-system change are mixed, as all indicators show synergies regarding cropland reduction but mixed behavior regarding deforestation and afforestation. A switch from conventional to extensive crop management seems to be a driving factor in these interconnections. Compared to these results, the scenarios taxing nitrogen application or deforestation show fewer and weaker synergies combined with more conflicts.

Despite its simplicity, this model and its scenario results offer insights and opportunities for future research about synergies and conflicts between multiple sustainability goals, especially greenhouse gas emissions, biodiversity loss, water use, and phosphorus as well as the potential of extensive farming.

Dedicated to

Brigitte Koch

(May 16, 1928 – October 11, 2020),

grandmother, storyteller, friend,

for her guidance and endless support

Contents

List of Figures

List of Tables

Abbreviations

ASI	Central, South, South-East, and East Asia (RoW model region)
ASM	Agricultural Sector Model
BDL	Biodiversity loss
C, Con	Conventional (management system)
C	Cropland (land type)
E, Ext	Extensive (management system)
F	Forest (land type)
FAO	Food and Agriculture Prganization of the United Nations
GHG	Greenhouse gas emissions (CO_2eq)
IIASA	International Institute for Applied Systems Analysis
IPBES	Intergovernmental Science-Policy Platform on Biodiversity and Ecosystem Services
IPCC	Intergovernmental Panel on Climate Change
Irr	Irrigated
LMC	Land-management change
LAM	Latin America (RoW model region)
LMC	Land-management change
LU	Land use
LUC	Land-use change
MAF	Middle East and Africa (RoW model region)
MDER	Minimum Dietary Energy Requirements
NAM	Northern America (RoW model region)
N, Nat	Natural (management system)
O	Organic (farming system)
O	Other natural land (land type)
OCE	Australia and New Zealand (Row model region)
p	Pasture (land type)
RF	Rainfed
RoW	Rest of the world
SDG	Sustainable Development Goal
SSP	Shared Socioeconomic Pathways
SSPDB	Shared Socioeconomic Pathways Database
TLU	Tropical Livestock Unit
U	Urban (land type,management system)

Model notation

Variables

In order of appearance.

Symbol	Description	Unit
W	Total welfare	1000 USD
$Q_{t,r,p}$	Quantity of any consumable good p sold in region r and period t	1000 t
$C_{t,r,c,m}$	Crop Area in region r and period t for crop c under management system m	1000 ha
$L_{t,r,l}$	Animals l raised in region r and period t	1000 heads
$P_{t,r,q}$	Amount of inputs processed through processes q in region r and period t	1000 t
$T_{t,r',r,p}$	Amount of products p shipped from exporter region r' to importer r in period t	1000 t
$S_{t,r,p}^{L/+/-}$	Storage level (L), input (+) and removal (-) of product p in period t and region r	1000 t
$E_{t,r,e}$	Extent of externalities e in region r and period t	units vary
$M_{t,r,t'}^{c}, M_{t,r,t'}^{l}$	Mix variable weighting historical crop (c) or livestock (l) mixes for region r, period t and historical period t'	1
$LU_{t,r,x}$	Land type x in period t in region r	1000 ha
$LUM_{t,r,x,m}$	Area of land type x in period t in region r under management m	1000 ha
$LC_{t,r,x,m,x',m'}$	LUC/LMC area from land type x under management m to land type x' under management m' in period t and region r	1000 ha
$I_{t,r,a}$	Extent of additional sustainability indicator a in period t and region r	1000 ha
R_{j}^{E}	Relative change between indicator j in base scenario and tax scenario E	1

Reoccuring Parameters

In order of appearance

Symbol	Description	Unit
$z_{r,p}$	Consumer price for product p in region r	$\mathrm{USD\,t^{-1}}$
$c^c_{r,c}$	Producer cost of crop c in region r	$\mathrm{USD\,ha^{-1}}$
c^m_m	Cost factor for crop management m	1
$c^l_{r,l}$	Producer cost of animal l in region r	$\mathrm{USD\,head^{-1}}$
$c^q_{r,q}$	Producer cost of process q in region r	$\mathrm{USD\,t^{-1}}$
t_e	Tax rate per unit of externality e	USD/unit of e
$y^c_{r,c,p}$	Yield of product p from crop c in region r	$\mathrm{t\,ha^{-1}}$
$y^m_{c,m}$	Yield factor for crop c under management m	1
$y^l_{r,l,p}$	Yield of product p from animal l in region r	$\mathrm{t\,head^{-1}}$
$y^q_{r,c,p}$	Yield of output/requirement of input p in process q in region r	$\mathrm{t\,t^{-1}}$

Reoccuring Indices

In order of appearance

Symbol	Description
t	Period
r	Region
c	Crop
p	Product
m	Management system
l	Animals
q	Process
e	Externalities
x	Land type
j	Indicators

Chapter 1

Introduction

Despite remaining inequalities, there is a global trend towards better lives for everyone, with the Human Development Index steadily rising, and multidimensional poverty and childhood mortality in turn shrinking (UNDP, 2018; Alkire et al., 2020; Hug et al., 2019). Overall, human development, especially in the last hundred years, has made enormous strides. At the same time, it has also had enormous impact on the environment. The release of anthropogenic greenhouse gases (GHG) is changing the climate at an unprecedented rate (IPCC, 2014). Large-scale land-use change and invasions into remaining undisturbed habitats are leading to an increasing loss of biodiversity (IPBES, 2019), considered to be the sixth mass extinction (Ceballos et al., 2015) and the first one to be attributed to humanity. These and other anthropogenic impacts have accumulated to such a degree that some suggest the start of a new geological epoch, the *Anthropocene* (Crutzen, 2002), named after humanity as the characterizing planet-shaping force.

In addition to this steady environmental deterioration, according to Rockström et al. (2009a), human influence may also lead to "abrupt environmental change within continental- to planetary-scale systems". More precisely, Rockström et al. (2009a) have identified nine biophysical thresholds, so-called *planetary boundaries*, for critical Earth system processes, "estimating the safe operating space for humanity with respect to the functioning of the Earth system". They suggest, if humanity aims at sustaining the relative environmental stability it has known and profited from so

far, to limit human impact on the associated sub-systems and processes so as to stay within these boundaries. If these boundaries are not respected and tipping points are reached, the Earth system may experience irreversible and rapid changes that will likely negatively affect most or all of humanity and other life on Earth (Rockström et al., 2009b). If adaptation to such changes is possible at all, it would likely be costly and hamper human development (UNEP, 2018, p. 22). This may affect less developed regions especially badly, as they are more exposed and more vulnerable (Hoegh-Guldberg et al., 2018, p. 244f.).

Because of this, both the positive trajectory of humanity and a sustainable life within the planetary boundaries are key to the 2015 UN Sustainable Development Goals (SDGs) for 2030. They aim at "end[ing] [...] hunger, in all [its] forms and dimensions, and to ensure that all human beings can fulfil their potential [...] in a healthy environment" while also "protect[ing] the planet from degradation, including through sustainable [...] production, sustainably managing its natural resources and taking urgent action on climate change, so that it can support the needs of the present and future generations" (UN, 2017).

While the UN (2017) does not directly name the concept of the planetary boundaries, working towards the SDGs is indivisibly linked to them. This is especially true for three SDGs focusing directly on the environment, namely SDGs 13, 14, and 15: climate action, life below water, and life on land. As defined by Rockström et al. (2009a), SDG 13 naturally links to a necessary planetary boundary on GHG emissions and anthropogenic climate change. SDG 14 is directly linked to the boundaries on ocean acidity, increasing due to CO_2 emissions, and flows of nitrogen and phosphorus into water bodies, affecting marine ecosystems. SDG 15 is directly linked to change in land use, especially through deforestation and cropland expansion, chemical pollution of soils, and biodiversity loss. Furthermore, SDG 6, clean water and sanitation, is linked to the boundary on global freshwater use. In addition, all of these boundaries are connected to SDG 2, zero hunger. This is because large scale agriculture is necessary to ensure good healthy lives and key to achieving SDG 2's food security

target. At the same time, land use is negatively affecting all Earth system processes associated with planetary boundaries (O'Neill et al., 2018; Campbell et al., 2017).

Including an update by Steffen et al. (2015), not all planetary boundaries have been defined with measurable values. Still, previous research has thoroughly assessed the current state of Earth system processes linked to each boundary, potential impacts of transgressing them, and possible ways to stay withing them. For some of the investigated Earth system processes and sub-systems, large-scale international research and policy cooperation exists, such as the Intergovernmental Panel on Climate Change (IPCC) or the Intergovernmental Science-Policy Platform on Biodiversity and Ecosystem Services (IPBES).
In comparison, relatively little previous research is available on the interconnection, synergies, and conflicts between sets of SDGs and the planetary boundaries. An exception is a relatively new model by Randers et al. (2019), *Earth3*, aiming at modeling sustainable development paths in line with all SDGs and within all planetary boundaries. Since it is critical to stay within all planetary boundaries (Rockström et al., 2009a), better knowledge of the interconnections between the associated Earth system processes is crucial to shape evidence based pathways into a more sustainable future, and more research in this direction is necessary.

While an ambitious project similar to *Earth3* by Randers et al. (2019) is vastly out of scope for a Master's thesis, this work's goal is to further our understanding of the interconnections between a set of the Earth system processes linked to planetary boundaries and affected by the agricultural sectors – an important sub-sector of human development, which is in the difficult position of balancing out several human needs and SDGs. Specifically, in this thesis, I build a simple agricultural sector model (ASM) to estimate several sectoral sustainability indicators associated with planetary boundaries: GHG emissions, biodiversity loss, land-use change (deforestation, afforestation, and cropland area), blue and gray fresh water use, and agricultural input of phosphorus and synthetic nitrogen. By running several scenarios, in each

forcing a different indicator to its possible minimum within set constraints, and assessing the changing levels of all the indicators, I try to answer the question:

How strong are synergies and conflicts between different planetary impacts of land use, particularly between climate change, biosphere integrity, biogeochemical flows of nitrogen and phosphorus, freshwater use, and land-system change?

To reflect the described conflict between several SDGs, a central constraint for the model is consumption at such a level that, in theory, food security and zero hunger are possible. Furthermore, I do not model all of the investigated planetary impacts in the same units as their planetary boundaries have been defined by Rockström et al. (2009a) but estimate proxies instead. For the climate system, they use atmospheric CO_2 concentration (ppm) or radiative forcing ($\mathrm{w\,m^{-2}}$). Instead, I model global land use emissions ($\mathrm{t\,CO_2eq}$). For biosphere integrity, Rockström et al. (2009a) use the extinction rate ($\mathrm{million^{-1}\,yr^{-1}}$), while I estimate the global ecosystem quality through areas (1000 ha) at different ecosystem quality levels (%) compared to wild systems. For nitrogen, I use the same approach as Rockström et al. (2009a), estimating the N_2 fixation from the atmosphere for agricultural use through synthetic fertilizer estimations (t). While I do not calculate the phosphorus run-off into the ocean directly, estimating agricultural inputs (t) can serve as proxy. For blue and gray water, I use the same indicator, water consumption ($\mathrm{m^3}$), as Rockström et al. (2009a). As the boundary for land-system change is an area limit of 15% of global ice-free land, here, too, I use the same indicator. Additionally, I investigate deforestation and afforestation.

I write the model using the *General Algebraic Modeling System* (GAMS), a system widely used for agricultural optimization problems and models, such as the *Common Agricultural Policy Regional Impact* (CAPRI) model, the *European Forest and Agricultural Sector Optimization Model* (EU-FASOM), the *Global Biosphere Manage-*

ment Model (GLOBIOM), or the *Model of Agricultural Production and its Impact on the Environment* (MAgPIE). Using the commercial CPLEX solver, GAMS solves the model as a linear programming problem.

Due to its simplicity, the model cannot reasonably estimate how close to or far from each respective boundary the agricultural impacts are. However, within the set parameters, I can use it to asses relative change in these indicators and estimate correlations. These results and this model can then form a basis and framework for future more in-depth work.

In chapter 2, I introduce the model, its core modules – consumption, production, and externalities –, equations, and the data used. Finally, I will discuss the resulting indicators for all scenarios in chapter 3. These findings are summarized in chapter 4.

Chapter 2

Model and Data

I estimate co-benefits and negative consequences of reducing agricultural pressure on the investigated Earth system processes using a partial-equilibrium agricultural sector model, maximizing agricultural welfare while taxing several negative externalities, as shown in (1):

$$\begin{aligned}\max\ W = &\sum_{t,r,p}\left(z_{r,p}\cdot Q_{t,r,p}\right) - \sum_{t,r,c,m}\left(c^{c}_{r,c}\cdot c^{m}_{m}\ \cdot C_{t,r,c,m}\right) - \sum_{t,r,l}\left(c^{l}_{r,l}\cdot L_{t,r,l}\right)\\ &- \sum_{t,r,q}\left(c^{q}_{r,q}\cdot P_{t,r,q}\right) - \sum_{t,r',r,p}\left(z_{r,p}\cdot 0.15\cdot T_{t,r',r,p}\right)\\ &- \sum_{t,r,p}\left(z_{r,p}\cdot\left(0.01\cdot\left(S^{+}_{t,r,p}+S^{-}_{t,r,p}\right)+0.03\cdot S^{L}_{t,r,p}\right)\right)\\ &- \sum_{t,r,e}\left(t_{e}\cdot E_{t,r,e}\right),\end{aligned} \tag{1}$$

where uppercase letters mark (with the exception of W) non-negative variables determined by the model, lowercase letters mark parameters fed into the model, and subscripts mark indices to be summed over. Going through the summands from left to right, W is the total welfare (1000 USD) produced, $Q_{t,r,p}$ is the quantity (1000 t) of any consumable good p sold in region r and period t at price z (USD t^{-1}), which is constant over time for any region r and product p; $C_{t,r,c,m}$ is the area (1000 ha) used in any region r and period t to grow crop c, utilizing management system m.

$c^c_{r,c}$ is the time-independent cost (USD ha^{-1}) per crop c in region r, which is modified through cost factor c^m_m, which is determined by the management system m; $L_{t,r,l}$ is the amount of animals l (1000 heads) raised in region r and period t, $c^l_{r,l}$ the associated time-independent cost; $P_{t,r,q}$ is the amount (1000 t) of input products processed in process q, region r and period t at cost $c^q_{r,q}$ (USD / input t); $T_{t,r',r,p}$ is the amount (1000 t) of products p shipped internationally from exporter region r' to the consuming or re-trading region r in period t; $S^L_{t,r,p}$ is the storage level (1000 t), $S^+_{t,r,p}$ and $S^-_{t,r,p}$ the amount of product p added to and taken from storage in region r and period t. Finally, $E_{t,r,e}$ summarizes the extent of the externalities e (units vary) in region r and period t taxed at rate t_e (USD / unit externality) in the model. The underlying assumptions, constraining equations, and data inputs will be further explained in the following sections of this chapter.

With this objective function, the model simulates a simple global production, consumption, and trade network. In this model, consumption is constrained by a corridor of minimum and maximum calorie consumption per capita. Production is constrained by available land for crop growth and livestock grazing; maximum annual land-use change (LUC); and historical land use (LU), crop and livestock-mix data. This will be further explained in sections 2.1 and 2.2, respectively.

The model covers 33 regions: the **EU-28 (EU) countries** on national levels and 5 aggregate Rest-of-the-Word (RoW) regions: Latin America (**LAM**), Northern America (**NAM**), Central, South and East Asia (**ASI**), Africa and West Asia (**MAF**), and large parts of Oceania (**OCE**). In turn, it does not cover non-EU Europe, including Russia, and many small island states. I choose the regions this way to ensure efficient data extraction and alignment, mostly from and between the Food and Agriculture Organization of the United Nations (FAO)'s FAOSTAT and the International Institue for Applied System Analysis (IIASA)'s Shared Socioecnomic Pathways (SSP) database, SSPDB. The regions and their FAOSTAT and SSPDB counterparts are shown in the supplementary material (see Appendix). To calculate parameters for these RoW regions, I, usually, sum over or average (without weight) data for sub-

Crop primary	apples, bananas, barley, beans, cassava, chickpeas (and other pulses), maize, millet, oil palm fruits*, olives, onions, oranges, potatoes, rapeseed, rice, sorghum, soybeans, sugarcane*, sunflower seeds, tomatoes, wheat
Livestock primary	beef, eggs, milk, pork, poultry
Process products	butter, feed*, olive oil, palm oil, rapeseed oil, skimmed milk, soy oil, sunflower oil

Table 1: Products covered by the model. * indicates products not for direct human consumption

regions. In few instances where no data is available for sub-regions, I use data for a selection of regional countries instead.

The temporal resolution is 5-year steps between **2015 and 2050**. **34 products** from crop production, livestock production, or resulting from product processing are covered, as listed in table 1. I choose this selection due to its global or regional importance, as these products supply the majority of calories consumed or are consumed in high amounts, based on data for 2015 from the FAO (2020, New Food Balances).

Based on land use, management systems, and land-use change, I calculate several sustainability impact indicators for the investigated Earth system processes: greenhouse gas (GHG) emissions through crop and livestock production, land-atmosphere carbon cycling, land-use change, and international trade; blue and gray freshwater use through crop production; land-use change through deforestation, afforestation and total cropland area; biodiversity loss (BDL) through land use and management; and interference with the nitrogen (N) and phosphorus (P) cycle through crop fertilization.

I investigate different scenarios, where in each a different negative externality is internalized through taxes. For each of these scenarios, I compare the resulting indicators to a base scenario without any taxes. The taxable externalities are **greenhouse gas emissions** (t CO_2eq), **biodiversity loss** (1000 ha), **synthetic nitrogen fertilizer application** (t), **phosphorus application** (t), **blue and gray freshwater use** (1000 m^3), and **deforestation** (1000 ha). Externalities and indicators will be further explained in section 2.3.

2.1 Consumption

Consumption $Q_{t,r,p}$, as only positive component in (1), is limited both by the availability of consumable products, as will be further discussed in section 2.2, and the caloric need in any region, as shown in (3):

$$n_{t,r} \cdot 1.1 \leq \frac{\sum_p (Q_{t,r,p} \cdot k_p)}{p_{t,r}} \leq n_{t,r} \cdot 1.8 \quad \forall t, r, \tag{2}$$

$$\text{where} \quad p_{t,r} = \sum_{a,g} p_{t,r,a,g}, \tag{3}$$

and where $n_{t,r}$ is the minimum dietary energy requirement (MDER, in kcal) of the population in region r in period t and k_p is the average amount of energy (1000 $\text{kcal}\,\text{t}^{-1}$) contained in consumable product p. I choose factors 1.1 and 1.8 to reflect unequal food distribution and food loss on the lower and wealthy consumption behavior on the upper end. $p_{t,r}$ is the total population, $p_{t,r,a,g}$ the number of people (millions) in age group a and of sex g in region r and period t, as projected in the SSPDB for SSP 2,"*Middle of the road*", (Riahi et al., 2017; KC & Lutz, 2017).
I estimate $n_{t,r}$ for each region r and period t as weighted average, as given in (4):

$$n_{t,r} = \frac{\sum_{a,g} (n_{a,g} \cdot p_{t,r,a,g})}{\sum_{a,g} p_{t,r,a,g}} \cdot 365, \tag{4}$$

where $n_{a,g}$ is the estimated daily calorie need per person of age a and sex g, based on recommendations for moderately active American citizens (U.S. Department of Health and Human Services & U.S. Department of Agriculture, 2015, appendix 2).
To fill gaps in the MDER table for ages 0–2, I extrapolate from the existing recommendations. Furthermore, to align age groups between the MDER table and the SSPDB population data, I form new age groups for the recommendations, assuming

the same recommendation for each age within an existing age group and averaging accordingly. For example, I calculate the MDER for the SSPDB aligned age group 30–34 for each sex as $n_g^{30\text{–}34} = (n_g^{26\text{–}30} + n_g^{31\text{–}35} \cdot 4)/5$. A full table of the adjusted age groups and resulting MDER estimates for all regions is available in the supplementary materials (see Appendix).

While, even without correctional factors, (3) ensures that the MDER for every person can be met, producing only exactly n_t^{global} per period would likely imply widespread undernourishment, due to e.g. food waste and distribution inequality (Hasegawa et al., 2019; Papargyropoulou et al., 2014). 10% additional consumption is a rough estimate to fulfill SDG 2 in the model while reflecting these problems in principle. In reality, it may be necessary to overproduce much more to counter current distribution inequalities.

At the other end of the spectrum, in wealthy countries where hunger is no major issue, food consumption is not unlimited. Looking at FAO (2020, New Food Balances) data for wealthy EU countries, I find supply as high as 3700–3900 $\mathrm{kcal\,capita^{-1}\,day^{-1}}$ in e.g. Austria, Belgium, or Ireland. Assuming that these mark the upper limit of average consumption and assuming a global average MDER of 2100, I estimate factor 1.8 for the upper limit.

I estimate the caloric content per ton of product p, k_p, as shown in 5:

$$k_p = \sum_{r'} \left(\frac{g_{r',p} \cdot 365}{m_{r',p}} \right) \cdot \frac{1000}{\sum_{r'} 1}, \tag{5}$$

where $g_{r',p}$ is is the food supply ($\mathrm{kcal\,capita^{-1}\,day^{-1}}$) and $m_{r,p}$ the food supply quantity ($\mathrm{kg\,capita^{-1}\,year^{-1}}$) of product p in region r'. While I calculate k_p for global use, r' is a subset of r depending on the specific product p. This varies, as some regions may show $m_{r,p} = 0$ for some products in the dataset. Furthermore, while (5) is straightforward in principle, for some regions and products, the data produces k_p many times higher than reference values from other sources, such as the U.S. Department of Agriculture (2020). To filter these outliers, I only considered region results for a product if $0 < \frac{g_{r',p} \cdot 365}{m_{r',p}} < 9000\,\mathrm{kcal\,kg^{-1}}$, resulting in global estimates as shown in table 2.

Apples	530.5	Bananas	615.3	Barley	2590
Beans	3401.3	Beef	1446.9	Butter	7347.4
Cassavar	1485.7	Chickpeas	3575.2	Eggs	1418.8
Feed	-	Maize	2924	Milk	547.1
Millet	3004.8	Oil palm fruit	-	Olives	1107.7
Olive oil	8805.6	Onions	381.6	Oranges	400.4
Palm oil	8801.0	Pork	2108.3	Potatoes	684.2
Poultry	1337.0	Rapeseed	2494.2	Rapeseed oil	8643.4
Rice	3035.7	Skimmed milk	205.1	Sorghum	3167
Soybeans	2745.5	Soy oil	8836.3	Sugarcane	-
Sunflower seeds	3115.7	Sunflower oil	8812.7	Tomatoes	236.2
Wheat	2834.0				

Table 2: kcal estimates per product ton ($\mathrm{kcal\,kg^{-1}}$), as calculated based on (FAO, 2020, New Food Balances). No data is given for products not meant for human consumption.

Besides $Q_{t,r,p}$, revenue and welfare also depend on the regional product price $z_{r,p}$ ($\mathrm{USD\,t^{-1}}$). These prices are estimated based on 2015 FAO (2020, Producer Prices) producer price data. As there are no regional aggregates available, I take a selection of countries for each RoW region to average their respective price data as RoW producer prices (ASI: China (mainland), Indonesia, Kazakhstan, Mongolia, Pakistan, Thailand; LAM: Argentina, Brazil, Chile, Colombia, Mexico, Paraguay, Peru; MAF: Algeria, Chad, Egypt, Iraq, Mali, Saudi Arabia, Yemen; NAM: Canada; OCE: Australia, New Zealand). Where no producer price data is available for a product and region, I use a continental (in the case of the EU-28 countries) or global average (for RoW regions or if no EU-28 average is available, as, for example, in the case of oil palms).

FAO (2020, Producer Prices) does not provide price data for processed goods, such as oils. To estimate these, I take global values and quantities of imported and exported goods from the FAO (2020, Crops and livestock products) trade dataset. Using these data, I calculate the value per traded quantity and average between import and export data to estimate the selling price of these processed goods. Testing this estimation method with 337 product-region combinations where producer price data is available shows that the price estimates from trade values may be as low as 8% and and as high

as 300% of the corresponding producer price. 80% of the estimates underestimate the price compared to their corresponding producer prices. As roughly 50% of the values underestimate the price by 40% or less, I correct the trade-based price estimates by factor 1.4.

I exclude skimmed milk and feed from this estimation process. Feed has a selling value of 0 as it is only intended for livestock consumption. Skimmed milk, while a result from processing milk into butter, is sold at the same price as unprocessed milk, as is typically done in German convenience stores. Furthermore, while price estimates for oil palm fruits and sugarcane are necessary for the cost estimates, as described in section 2.2, similar to feed, I set their consumer price to 0, as they are not meant for direct human consumption.

2.2 Production

Any product that is consumed in (1) first needs to be produced from cropland, livestock, or through processes. Further, in an optimized model, any product that is produced is also consumed, directly or indirectly. However, this does not necessitate that a product must be consumed in the same period or region it was produced, due to trade and storage options. For this model, these aspects are reflected in the product balance equation (6):

$$\begin{aligned} Q_{t,r,p} = &\sum_{c,m} \left(y^{c}_{r,c,p} \cdot y^{m}_{c,m} \cdot C_{t,r,c,m}\right) + \sum_{l} \left(y^{l}_{r,l,p} \cdot L_{t,r,l}\right) + \sum_{q} \left(y^{q}_{r,q,p} \cdot P_{t,r,q}\right) \\ &+ \sum_{r'} \left(T_{t,r',r,p} - T_{t,r,r',p}\right) + S^{-}_{t,r,p} - S^{+}_{t,r,p} \quad \forall t, r, p, \end{aligned} \tag{6}$$

where $y^{c}_{r,c,p}$ is the yield ($\mathrm{t\,ha^{-1}}$) of crop c's primary product p from area $C_{t,r,c,m}$ in region r and period t, amplified or reduced by the yield factor $y^{m}_{c,m}$, depending on the used management system m. Livestock yield ($\mathrm{t\,head^{-1}}$) $y^{l}_{r,l.p}$ can be both positive (primary livestock products) and negative (feed products consumed by livestock). Process yields $y^{q}_{r,q,p}$ ($\mathrm{t\,t^{-1}}$ produced / processed) are negative for input products and

positive for outputs of process q. The trade term is positive if region r is a net importer and negative if it is a net exporter in period t. Lastly, I add products taken from Storage S^- (1000 t) to the balance while subtracting products put into storage S^+ (1000 t).

2.2.1 Crop production

Crop production affects overall welfare by limiting the available product amount in (6) and through production costs in (1). Crop production is limited by available land.

Crop yield

I estimate crop yields $y^c_{r,c,p}$ based on FAO (2020, Crops) yield data, averaged over period 2010–2014 per crop c and region r. In this model, I assume this baseline yield to be time independent. If there is no yield data available in the used dataset, I estimate yield in this region to be 0 for this crop. In case of the EU-28 countries, I make an exception if price data, as described in section 2.1, is available on national level. In that case, I use the EU average yield for this region. This only affects apples and beans in Austria, and beans in Great Britain and Northern Island.

$$y^m_{c,m} = g^y_m \cdot i^y_m \tag{7}$$

The management yield factor $y^m_{c,m}$ is based on two components, as shown in (7), the general component g^y_m, comprising e.g. fertilizer inputs and pest control, and the water component i^y_m. g^y_m comprises three fundamental production systems: **conventional**, **organic**, and **extensive** farming. i^y_m expands these three systems by either adding artifical **irrigation** (Irr) or limiting them to **rainfed** (RF) production. However, extensive farming can by definition only be rainfed (Reidsma et al., 2006). As such, the model covers five different crop management systems.

I consider the rainfed conventional management system to be the baseline, where both g^y_m and $i^y_m = 1$, resulting in $y^m_{c,m} = 1$. Organic farming systems abstain from many synthetic inputs, resulting in on average lower yields. While there is great variability

between yields from different organically managed farms, dependent on crop types, regions, and more, for simplicity, I assume a single factor of 0.8 independent of these aspects, in accordance with estimates by Ponti et al. (2012). Extensive farming is a farming system of low external inputs and disturbances of the environment. Reidsma et al. (2006) describe different extensive variations of conventional or organic farming as e.g. traditional farms or permaculture systems. Such systems are even further removed from the output-focused conventional farming systems than the described organic management. For example, fertilizer and pest control inputs are significantly lower than in organic systems (Reidsma et al., 2006). As these inputs are expensive and only used to increase yield and due to the lack of yield data in large scale extensive farms, I estimate the yield factor of extensive farming based on input cost ranges taken from the system definitions by Reidsma et al. (2006), where an intensive system (organic or conventional) takes between 80 and 250 USD per hectare and an extensive system less than 80 USD per hectare. Assuming a uniform cost distribution, averaging extensive input cost at 40 USD and organic intensive cost at 165 USD, I estimate yields from extensive organic systems to be $\frac{40}{165} = 24\%$ of organic base yields. As I estimate organic yields to be 80% of the baseline conventional yields, my estimation for extensive yields is 19%.

To estimate i_m^y, I average yield changes in artificially irrigated systems compared to rainfed ones, as given in (8):

$$i_m^y = \frac{\sum_c \frac{y_c^{\mathrm{Irr}}}{y_c^{\mathrm{RF}}}}{\sum_c 1}, \tag{8}$$

where y_c^{Irr} and y_c^{RF} are the irrigated and rainfed yield for nine crops, as presented by Mekonnen & Hoekstra (2011, table 8). By calculating the unweighted average of these crop-specific yield factors, I receive $i_m^y = 1.38$, as shown in table 3. The resulting management-dependent yield factors y_m^m are summarized in table 4.
If the global average for a crop's blue water footprint equals 0, as estimated by (Mekonnen & Hoekstra, 2011, appendix IV), I set irrigated yield to 0, as this crop apparently

	Yield ($\mathrm{t\,ha^{-1}}$)		
Crop	Rainfed	Irrigated	Irr-RF-Factor
Wheat	2.48	3.31	1.33
Maize	4.07	6.01	1.48
Rice	2.69	4.67	1.74
Apples	8.93	15.91	1.78
Soybean	2.22	2.48	1.12
Sugarcane	58.7	71.17	1.21
Coffee	0.68	0.98	1.44
Rapeseed	1.63	1.23	0.75
Cotton	1.35	2.16	1.6
Average			**1.38**

Table 3: Comparison of yield data for rainfed and irrigated crops, averaged 1996–2005, taken from Mekonnen & Hoekstra (2011).

Factor	C-RF	C-Irr	O-RF	O-Irr	E	N	U
Yield y_m^m	1	1.38	0.8	1.104	0.19	-	-
Cost c_m^m	1	1.2	0.9	1.08	0.6	-	-
Water (blue) $w_m^{m,b}$	0	1.38	0	1.104	0	-	-
Water (gray) $w_m^{m,g}$	1	1.1	0.8	0.9	0	-	-
Nitrogen $i_r^{m,N}$	1	1.1	0	0	0	-	-
Phosphorus $i_r^{m,P}$	1	1.1	0.8	0.9	0.1	-	-
Emissions (rice cultivation) $e_{c,m,e}^m$	1	1.38	0.8	1.104	0.19	-	-
Emissions (synthetic N) $e_{c,m,e}^m$	1	1.1	0	0	0	-	-
Emissions (manure on soil) $e_{c,m,e}^m$	1	1.1	1.2	1.2	0.1	-	-
Emissions (crop residues) $e_{c,m,e}^m$	1	1.38	0.8	1.104	0.19	-	-
Biodiversity loss b_m^{C}	0.9	0.95	0.8	0.85	0.65	-	-
Biodiversity loss b_m^{P}	0.8	-	-	-	0.6	0	-
Biodiversity loss $b_m^{\mathrm{F/O}}$	-	-	-	-	-	0	-
Biodiversity loss b_m^{U}	-	-	-	-	-	-	1
$\mathrm{TLU\,ha^{-1}}$ pasture u_m^m	2	-	-	-	1	0.3	-

Table 4: Summary of estimated and calculated management factors for conventional (C) and organic (O), rainfed (RF) or artificially irrigated (Irr), and extensive (E) systems as well as natural (N) and urban (U) environments. All factors are for cropland except biodiversity loss, where the landtype is indicated (cropland (C), pasture (P), forest (F), other natural land (O), and urban (U)), and TLU pasture density. Biodiversity loss shares and TLU pasture density taken from Reidsma et al. (2006).

never profits from irrigation. In the dataset used, this applies only to oil palms.

Crop costs

While products are priced by ton, crop production cost is calculated based on the crop area $C_{t,r,c,m}$. Cost per area further depends on a regional baseline factor $c^c_{r,c}$ (USD ha^{-1}) and a management factor c^m_m. Based on the assumption that production cost and consumer prices are balanced, I estimate baseline cost as given in (9):

$$c^c_{r,c} = z_{r,p} \cdot y^c_{r,c,p}, \tag{9}$$

where $z_{r,p}$ is the consumer price in region r for product p, and $y^c_{r,c,p}$ is the associated product yield from crop c. Crop data and underlying calculations are provided in the supplementary material (see Appendix).

As shown in (1), depending on the applied crop management system m, I modify this baseline with a management factor c^m_m, comprising a general term and an irrigation term, as given in (10):

$$c^m_m = g^c_m \cdot i^c_m, \tag{10}$$

where g^c_m is the general term, reflecting the fundamental management system and especially the cost of inputs, such as fertilizer and pesticides, and i^c_m depends on the chosen irrigation system or lack thereof.

As for yield calculations, the baseline management system with $g^c_m = 1, i^c_m = 1, c^m_{c,m} = 1$ is a conventional rainfed system. For organic or extensive systems, I assume g^c_m to be 0.9 and 0.6, respectively. These are rough estimates based on the assumption that these systems use fewer, cheaper inputs, but have to make up for their lower efficiency through increased labor investments. Due to the different inputs and labor-requirements, costs might even be higher per hectare than in an efficient conventional system. However, organic products often sell at higher price margins (Sgroi et al., 2015), which is not reflected directly in the price calculation of this model. To balance this out, I lower cost of organic systems below conventional.

As for i_m^c, irrigation is associated with higher costs than rainfed systems. Based on an estimate for maize irrigation in Tanzania by FAO (1997) compared to the baseline cost estimate for maize in the Africa and Middle East region in this thesis, a cost factor of 1.2 is assumed for irrigated systems compared to the baseline rainfed system. The resulting management dependent cost factors c_m^m are summarized in table 4.

Crop mix

Since a simple ASM without demand function, as created for this thesis, would likely specialize on few products with a relatively good profit margin and ignore many other, in reality, important products, I ensure a more realistic production and consumption behavior through crop-mix restriction (11):

$$\sum_m C_{t,r,c,m} = \sum_{t'} \left(m^c_{t',r,c} \cdot M^c_{t,r,t'} \right) \quad \forall t, r, c, \tag{11}$$

where $m^c_{t',r,c}$ is historical (FAO, 2020, Crops) crop-mix data comprising area amounts (ha) for crop c in region r and historical period $1995 \leq t' \leq 2014$, and crop-mix variable $M^c_{t,r,t'}$, which applies these historical amounts in full or in parts to the modeled periods t: If any of the historical crops c in region r are to be planted in period t again, $M^c_{t,r,t'} > 0$ is required for at least one t'. This allows crop c to be grown, but enforces at the same time all other crops c from period t' to be grown according to their historical shares. The function is not enforced for crops without history in region r, allowing them to be freely added next to potential historical crop mixes if other constraints do not apply. However, as yield data is linked to historical values as well and usually only exists based on them, it is very unlikely that a crop without historical precedent is grown in a new region in this model.

2.2.2 Livestock production

Livestock production affects welfare indirectly through the products it feeds into the product balance (6) as well as those it takes from it as feed and directly through the cost of any animal, as shown in (1).

Livestock yield

When calculating livestock yield, cost, and impacts, for simplicity reasons, I do not discern different specialized sub-species, such as broiler and layer chickens. For the investigated livestock products, I use FAO (2020, Livestock Primary) livestock yield ($\mathrm{t\,head^{-1}}$) data for 2014 and, where necessary, apply it to a single animal type which provides both milk and beef or eggs and poultry, respectively. For the RoW regions, I calculate yield estimates as unweighted average between the yield data for the FAO sub-regions.

While livestock produces primary livestock products, it also consumes feed. This feed consumption is expressed as negative yield term for feed $y_{r,l}^{l,\mathrm{feed}}$ ($\mathrm{t\,head^{-1}}$), an aggregate product including several crop and livestock primary products typically used for feeding, as shown in table 5. Due to its negative sign, feed is removed from the product balance (6) per animal l kept in period t and region r.
To estimate the non-pasture feed needed per animal, I use FAO (2020, New Food Balances) data on product feed use in 2014. Since the energy in the animal products is sourced from the feed, I assume that higher product tonnage correlates with higher feed intake. Based on this assumption, I estimate the feed necessary per livestock type l as shown in (12):

$$y_{r,l}^{l,\mathrm{feed}} = -\left(\frac{\sum_{p'} f_{r,p'}}{\sum_{p} x_{r,p}} \cdot \sum_{p} y_{r,l,p}^{l}\right), \tag{12}$$

where $f_{r,p'}$ is the amount of p' documented as feed and $x_{r,p}$ is the amount of livestock primary product p produced in region r according to the FAO (2020, New Food Balances; Livestock Primary) dataset. As the fraction provides $\mathrm{t\,t^{-1}}$ feed / livestock product, summing over the different product yields $y_{r,l,p}^{l}$ associated with livestock type l provides the regional $y_{r,l}^{l,\mathrm{feed}}$.

Crop	Share [%]	Scaled share [%]	Cost average [USD/t]	Weighted Cost [USD/t]
Maize	51	52	427.4	221.7
Wheat	11	11	304.2	33.2
Cassava	8	8	486.2	40.9
Milk	7	7	482.4	33.0
Barley	6	6	297.9	19.2
Rice	4	4	1531.7	23.6
Sugarcane	3	4	135.6	4.8
Potatoes	3	3	402.4	11.3
Sorghum	2	2	297.8	6.8
Soybeans	2	2	621.9	11.1
Chickpeas	1	1	962.2	6.3
Average				**411.9**

Table 5: Most import global feed shares and cost estimation for c^f, based on FAO (2020, New Food Balances, Producer Prices) data.

Livestock costs

Assuming a balance between production cost and consumer price, corrected for profit loss due to products being used as feed instead of for consumer consumption, I estimate the cost per animal l and region r, $c^l_{r,l}$, as shown in (13):

$$c_{r,l} = \sum_p \left(z_{r,p} \cdot y^l_{r,l,p}\right) - y^{l,\text{feed}}_{r,l} \cdot c^f, \tag{13}$$

where c^f is a global cost estimate per ton of feed. To estimate this global cost, I calculate the global and regional shares of different feed products to assess their importance based on 2014 FAO (2020, New Food Balances) data. Ignoring less important food products, I scale the selected shares to a total 100% and, based on the global average cost per product ton, calculated with FAO (2020, Producer Prices) data for 2015, estimate the global feed cost $c^f = 411.9\,\text{USD}\,\text{t}^{-1}$, as shown in table 5.
For some regions, this c^f leads to very low or negative $c^l_{r,l}$ for cattle, effectively subsidizing cattle production in these regions. As this is not an intended effect, cattle raising costs for these regions is set manually to a still comparatively low $300\,\text{USD}\,\text{head}^{-1}$. Furthermore, while I use this mix to estimate average feed and regional livestock pro-

duction cost, I do not enforce the mix itself in the model, leaving it free to find an alternative, more efficient feed mix.

Livestock mix

Analogous to crop mix, I implement a livestock mix function to keep the model from unrealistically specializing in a single livestock type, as shown in (14):

$$L_{t,r,l} = \sum_{t'} \left(m^{l}_{t',r,l} \cdot M^{l}_{t,r,t'} \right) \quad \forall t, r, l, \tag{14}$$

where $m^{l}_{t',r,l}$ is historical FAO (2020, Live Animals) livestock-mix data comprising stock numbers (heads) for livestock types l in region r and historical period $1995 \leq t' \leq 2014$. Livestock-mix variable $M^{c}_{t,r,t'}$ weights these historical data and applies them to the modeled periods t, as explained for the crop mix in sub-section 2.2.1.

2.2.3 Land constraints

The limiting factor in crop production is the available land, as shown in (15):

$$a_r = \sum_{x} LU_{t,r,x} \qquad \forall t, r, \tag{15}$$

$$\text{where } LU^{c}_{t,r} = \sum_{c,m} C_{t,r,c,m}, \quad LU^{p}_{t,r} = \sum_{m} LUM^{p}_{t,r,m} \qquad \forall t, r, \tag{16}$$

and where a_r is the total land area in region r based on 2010 FAO (2020, Land Use) data, $LU_{t,r,x}$ is the land use (1000 ha) in region r and period t per land type x (cropland c, pasture p, forest f, other natural land o, and urban and other artificial land u), and, in the case of cropland and pasture, m are the available management systems. $LUM_{t,r,x,m}$ is the area (1000 ha) of land type x under management m in period t and region r.

Similarly, livestock production is affected by the land-use conflict in (15) in two ways, as livestock requires feed grown on cropland as well as, for cattle and chickens, a

Region	Source regions	Cattle	Pigs	Chickens
EU-28	OECD	0.9	0.25	0.01
ASI	East and South East Asia [*Sic*], South Asia	0.575	0.225	0.01
LAM	Carribbean [*Sic*], Central America, South America	0.667	0.233	0.01
MAF	Africa South of Sahara, Near East, Near East North Africa, South Africa	0.613	0.213	0.01
NAM	North America	1	0.25	0.01
OCE	OECD	0.9	0.25	0.01

Table 6: Regional TLU estimates based on Chilonda & Otte (2006)

minimum amount of pasture, as shown in (17):

$$\sum_{m} \left(LUM^{p}_{t,r,m} \cdot u^{m}_{m} \right) \geq \sum_{l'} \left(L_{t,r,l'} \cdot u^{l}_{r,l'} \right) \quad \forall t, r, \tag{17}$$

where u^{m}_{m} is the livestock density on pasture ($\mathrm{TLU\,ha^{-1}}$), as defined by Reidsma et al. (2006) for different pasture management systems m and summarized in table 4, and $u^{l}_{r,l'}$ is the tropical livestock unit (TLU) for pasture dependent livestock type l' in region r. $u^{l}_{r,l}$ estimates are based on calculations by Chilonda & Otte (2006), where, depending on the model region, I average several source values to better reflect different realities, as shown in table 6.

I constrain land use in three ways: I use land shares from Climate Change Initiative Land Cover data (CCI_LC) provided by the FAO (2020, Land Cover) for reference period 2010 to initialize land cover in the model's first time step, 2015 (full table in supplementary material, see Appendix); I limit maximum growth and loss of any land type $LU_{t,r,x}$ per time step with a land-use change corridor, at the same time enforcing a minimum share of land type by 2050; and I enforce population-based growth of urban and other artificial areas $LU^{u}_{t,r}$. I use (18) and (19) to both initialize 2015

land-use values and to describe the allowed LUC corridor for following periods:

$$lu_{2010,r,x'} \cdot 0.95 \leq LU_{2015,r,x'} \leq lu_{2010,r,x'} \cdot 1.1 \qquad \forall r \qquad (18)$$

$$\text{and} \quad LU_{t-1,r,x'} \cdot 0.95 \leq LU_{t,r,x'} \leq LU_{t-1,r,x'} \cdot 1.1 \qquad \forall t, r, \qquad (19)$$

where $x' = [c, p, f, o]$ is the set of possible land types x, excluding urban, and $lu_{2010,r,x}$ is the reference FAO (2020, Land Cover) LU data for land type x in region r in 2010. I arbitrarily choose 5% maximum loss and 10% maximum gain per land type, region, and time step compared to the time step before $(t' - 1)$, as these values allow for large scale changes over time (up to 44% loss and 114% gain of any land type by 2050 compared to 2010, also depending on initial land distribution) and seem feasible per time step. Furthermore, choosing the corridor too narrowly would rob the model of much of its flexibility.

For urban evolution, I assume that, in general, urban area grows linearly with population numbers and that, even in the case of shrinking population, urban area stays at least on the current level, as shown in (20) and (21). Furthermore, maximum urban growth is limited by the assumption that urban population density will not fall below 50% of its 2010 value, $\frac{p_{2010,r}}{LU^u_{2010,r}}$:

$$\frac{lu^u_{2010,r}}{p_{2010,r}} \cdot p_{t,r} \leq LU^u_{t,r} \leq \frac{lu^u_{2010,r}}{p_{2010,r}} \cdot p_{t,r} \cdot 2 \qquad \forall t, r \qquad (20)$$

$$lu^u_{2010,r} \leq LU^u_{t-1,r} \leq LU^u_{t,r} \qquad \forall t, r, \qquad (21)$$

where $p_{t',r}$ is the total population (millions) in region r and period $t' = [2010, t]$, as projected in the SSPDB for SSP 2,"*Middle of the road*" (Riahi et al., 2017; KC & Lutz, 2017).

2.2.4 Processes

The third way to produce products in this model is through processing primary crop and livestock products into secondary ones. This affects product balance (6)

Input	Output(s)	Input	Output(s)
Milk	Butter, Skimmed milk	Olives	Olive oil
Oil palm fruits	Palm oil	Rapeseeds	Rapeseed oil, feed (cake)
Soybeans	Soy oil, feed (cake)	Sunflower seeds	Sunflower oil, feed (cake)

Table 7: Main product processes

twofold, by adding process outputs and removing process inputs through yield $y^q_{r,q,p}$, and welfare (1) due to process costs $c^q_{r,q}$. A full table with all process parameters is provided in the supplementary material (see Appendix).

Process yield

Process variable $P_{t,r,q}$ counts processes processing 1000 t of the respective input product. Hence, process requirements for all input products i is $y^q_{r,q,i} = -1$.
Overall, there are 17 processes in the model, of which 11 turn products most commonly used for feeding, as described in section 2.2.2 and shown in table 5, into feed at 100% efficiency. The remaining six processes produce regionally varying yields of seven consumable goods as well as feed as by-product, as shown in table 7.
For the oil processes, I determine $y^q_{r,q,p}$ as shown in (22):

$$y^q_{r,q,p} = \frac{\hat{p}_{2013,r,p}}{\hat{p}_{2013,r,i}}, \tag{22}$$

where $\hat{p}_{2013,r,p}$ is the production quantity (t) of the process output product and $\hat{p}_{2013,r,i}$ is the processed quantity (t) of the process input product, based on (FAO, 2020, Commodity Balances - Crops Primary Equivalent) data for 2013 in region r. For palm oil, no data on the input crop, oil palm fruit, is available in the commodity balances database. To fill this gap, I substitute the production amount per region from the (FAO, 2020, Crops) crops database. To estimate the processing share of crop production $p'_{t,r,c}$, I compare available crop production and processing data for other oil crops. Based on this, I estimate that, on average, 82% of produced oil palm fruits are processed and substitute $\hat{p}_{2013,r,\text{oil palm fruit}} = 0.82 \cdot p'_{t,r,\text{oil palm fruit}}$ in (22) to estimate $y^q_{r,q,p}$ for palm oil production.

For the butter process, I assume uniform global process efficiency and estimate it following steps outlined by Lambert (1988) and summarized in (23) and (24):

$$y^b = \frac{\left(1 - y^{m'}\right) \cdot f^c}{f^b}, \tag{23}$$

$$\text{with} \quad y^{m'} = \frac{f^c - f^m}{f^c - f^{m'}}, \tag{24}$$

where f^x, with $x = [m, m', c, b]$, is the fat content of unprocessed milk m, skimmed milk m', cream c, as intermediate production step, and butter b. Assuming $f^m = 4\%$, $f^{m'} = 1.5\%$, $f^c = 40\%$, and $f^b = 80\%$, I estimate $y^{m'} = 0.935\,\mathrm{t\,t^{-1}}$ skimmed milk and $y^b = 0.0325\,\mathrm{t\,t^{-1}}$ butter yield per processed ton milk.

Process cost

Similar to livestock and crop production costs, I estimate process costs based on the estimated consumer price $z_{r,p}$ per ton of process output product $\dot{p}$, estimated as explained in section 2.1, the process yield efficiency $y^q_{r,q,\dot{p}}$ ($\mathrm{t\,t^{-1}}$) and the cost of the processed input $c^i_{r,i}$. As process "yield", i.e. the input requirement, for the input product is defined as $y^q_{r,q,i} = -1$, process cost is expressed as shown in: (25)

$$c^q_{r,q} = \sum_p \left(z_{r,p} \cdot y^q_{r,q,p}\right), \quad \text{with } p = [\dot{p}, i]. \tag{25}$$

As such, both input cost and output price are considered. Furthermore, in the special case of the butter process, where two consumer products, i.e. butter and skimmed milk, are produced, both product prices and yield efficiencies are taken into consideration. Feed, on the other hand, doesn't have a cost. As such, it is not adding to the process cost, neither as by-product nor if it is the sole output product.

In some cases, the cost correction turns process costs negative for some regions and processes q'. For these, I estimate process cost as global cost average between regions with $c^q_{r,q'} > 0$.

2.2.5 Trade and Storage

Trade allows for a product produced in one region to be consumed or processed in another, while storage does the same for periods.

Trade

The only restriction on trade is the product balance (6), where the upper limit for exports from region r is the total available product amount in r and the upper limit for imports to r is the sum of available products in all other regions r'. For simplicity reasons, I allow trade between two regions to go to 0 and do not set historical trade routes as any kind of baseline.
I estimate trade cost as a share of the import value ($\mathrm{USD\,t^{-1}}$), as described by the United Nations Conference on Trade and Development (2017, Chp. 3). For simplicity, I assume the global average of 15 % of the regional product price $z_{r,p}$ for all trade, independent of the trading partners. For products not meant for direct human consumption, no $z_{r,p}$ exists. For these, I assume a flat transport cost.

Storage

Storage space is unlimited in this model, so that $S^L_{t,r,p}$ is only limited by product availability and minimum consumption, as they limit the amount $S^+_{t,r,p}$ that can be added to the storage in region r and period t, as shown in (26):

$$S^L_{t,r,p} = S^L_{t-1,r,p} + S^+_{t,r,p} - S^-_{t,r,p} \quad \forall t, r, p, \tag{26}$$

where $S^L_{t-1,r,p}$ is the sto rage level in the previous period (0, if $t = 2015$). Furthermore, to reflect product perishableness, products can only be stored for one period, as shown in (27):

$$S^-_{t,r,p} \geq S^+_{t-1,r,p} \quad \forall t, r, p. \tag{27}$$

Storage combines two different cost types. For $S^+_{t,r,p}$ and $S^-_{t,r,p}$, I consider transport to and from storage. For $S^L_{t,r,p}$, I assume rent and cooling to be important cost factors.

In both of these cases, I assume these costs to be only a fraction of international trade costs, which combines these factors on a larger scale, e.g. longer distances. Because of this, I estimate the cost for the storage transport process to be 1% of $z_{r,p}$ and 3% for the storage period.

2.3 Externalities and Sustainability Indicators

The final term in (1) internalizes externality costs through taxes. These externalities are GHG emissions, biodiversity loss, deforestation, blue and gray freshwater use, synthetic nitrogen fixation, and phosphorus pollution (proxied through their application). In addition to their cost, each externality's global cumulative level across the period 2015–2050 is also a sustainability impact indicator for the modeled agricultural system.

By default, I set all taxes to 0, defining the baseline run. In six follow-up runs, I tax one of the externalities with a prohibitively large cost per externality unit to highly incentivize system choices that minimize the taxed externality to investigate the lowest possible levels each indicator can reach and how this affects other indicators.

2.3.1 Greenhouse gas emissions

I estimate global GHG emissions per period t as sum of emissions from crop management, livestock, export transports, land-type specific emissions or uptake, and carbon release due to land-use change, as shown in 28:

$$\begin{aligned} E_{t,r}^{\mathrm{CO_2eq}} = &\sum_{c,m,e} \left(e_{r,c,e}^{c} \cdot e_{c,m,e}^{m} \cdot C_{t,r,c,m}\right) + \sum_{l} \left(e_{r,l}^{l} \cdot L_{t,r,l}\right) + \sum_{r',p} \left(e^{t} \cdot d_{r,r'} \cdot T_{t,r,r',p}\right) \\ &+ \sum_{x} \left(e_{r,x}^{x} \cdot LU_{t,r,x}\right) + \sum_{x,x'} \left(e_{r,x,x'}^{xc} \cdot LUC_{t,r,x,x'}\right) \quad \forall t, r, \end{aligned} \tag{28}$$

where $e_{r,c,e}^{c}$ is the crop emission factor ($\mathrm{t\,CO_2eq\,1000ha^{-1}}$) for emission type e and crop c in region r, $e_{c,m,e}^{m}$ is the associated management factor; $e_{r,l}^{l}$ is the total emissions ($\mathrm{t\,CO_2eq\,1000\,heads^{-1}}$) per livestock type l in region r; e^{t} is the trade distance emis-

sions ($\mathrm{t\,CO_2eq\,Mt\text{-}km^{-1}}$) and $d_{r,r'}$ the trade distance (1000 km) between two trading regions r, r'; $e^{x}_{r,x}$ is the land type specific emissions ($\mathrm{t\,CO_2eq\,1000\,ha^{-1}}$) per region r; and $e^{xc}_{r,x,x'}$ is the emission factor ($\mathrm{t\,CO_2eq\,1000\,ha^{-1}}$) for land-use change from land type x to land type x' in region r, dependent on land-use-change variable $LUC_{t,r,x,x'}$.

Crop emissions

For crop emissions, the emission types e include emissions from manure on soil, synthetic fertilizers, rice cultivation, and crop residues. Assuming uniform distribution, I estimate crop emissions based on FAO (2020, Emissions - Agriculture, Land Use, Crops) data for 2015 by dividing total emissions per type e by the total cropland area, with the exception of rice cultivation emissions, where I divide by the total rice area. Naturally, rice cultivation emissions are set to 0 for any crop but rice. Where no data is available, I use the global average for this emission type. This only applies to regions historically void of rice.

$e^{m}_{c,m,e}$ is the associated crop management factor, as shown in table 4, amplifying or reducing crop emissions. The GHG factor for synthetic fertilizer use is 0 for extensive and organic management systems, as these systems minimize this type of input by definition (Reidsma et al., 2006), 1 for rainfed and 1.1 for irrigated conventional systems, respectively, where I assume an increase with increasing yield. The factor for manure application is assumed to be 0.1 for extensive systems, as they use little, not necessarily no inputs at all (Reidsma et al., 2006). For organic systems, I assume 1.2 and 1.3 for rainfed and irrigated management, respectively, to make up for parts of the synthetic fertilizer reduction while also recognizing that the GHG impact per hectare is, in general, assumed to be lower for organic systems compared to conventional ones (Tuomisto et al., 2012). For conventional systems, I assume the factor to be 1 for rainfed and 1.1 for irrigated systems, as the former is the baseline and the latter's increased yield likely implies higher nutrient needs. I assume crop residues to directly correlate with yield. As such, I use the management specific yield factor as emission factor for residues as well. Similarly, for emissions from rice cultivation,

the factor is equal to the management specific yield factor if the crop is rice and 0 if it is not. All crop emission factors are provided in the supplementary material (see Appendix).

Livestock emissions

For Livestock, I use FAO (2020, Emissions - Agriculture) data on three emission types e, enteric fermentation, manure management, and manure left on pasture, combined with animal stock $\hat{l}_{r,l}$ for 2015, by livestock type l and region r. I estimate $e^l_{r,l}$ as shown in (29)

$$e^l_{r,l} = \frac{\sum_e \hat{e}_{r,l,e}}{\hat{l}_{r,l}}, \tag{29}$$

where $\hat{e}_{r,e,l}$ is the total amount of emissions of type e associated with livestock type l.

Trade emissions

I estimate the GHG footprint of trade based on the distance between trading partners, the assumed mix of transport methods, and estimated emissions per t-km of each transport method. For trade distances, I use geo data accumulated by Georg (2020), automatically centered in most regions, with the exception of NAM, OCE, and MAF, where I estimated Minneapolis, Melbourne, and Khartum, respectively, to roughly mark the center of their respective regions. A table with all distances is provided in the supplementary materials (see Appendix).

I estimate the mix of transport methods for all EU-28 countries and the additional regions uniformly by assuming globally similar mixes as well as shares of intra- and extra-regional trade. The mix estimate is based on EUROSTAT (2020a,b) data regarding transport mode shares for intra-EU and extra-EU trade in 2015 and 2019, respectively. For transport emissions ($\mathrm{t\,CO_2eq\,Mt\text{-}km^{-1}}$) by mode, I use data from Weber & Matthews (2008), averaging their estimates for container and bulk transport to get a single value for international water transport. The final $\mathrm{t\,CO_2eq\,Mt\text{-}km^{-1}}$ estimate results from a weighted average of extra-EU and intra-EU transport emissions, weighted 40:60, based on EUROSTAT (2020c) data, and amounts to roughly

Method	CO_2eq	Intra [%]	Intra [CO_2eq]	Extra [%]	Extra [CO_2eq]	Average 60 In:40 Ex [CO_2eq]
Sea	12.5	-	-	81	10.1	4.1
Air	680	-	-	1.7	11.5	4.6
Road	180	75.3	135.5	14.4	26	91.7
Rail	18	18.2	3.3	2.8	0.5	2.2
Water (intra)	21	6.5	1.4	-	-	0.8
Total						**103.4**

Table 8: Global average trade emissions (CO_2eq Mt-km^{-1}) calculated as 60:40 weighted average between intra (In) and extra (Ex) regional trade emissions per transport type, based on share of t-km data from EUROSTAT (2020a,b) and CO_2eq Mt-km^{-1} estimates from Weber & Matthews (2008). Average weights based on EUROSTAT (2020c) data. Original data includes 2.4 % other for extra-EU-27 trade. These are left out, the remaining methods are scaled to 100 %.

103.4 t CO_2eq Mt-km^{-1}, as shown in table 8.

Land-use emissions

Based on the general land type, I estimate consistent annual GHG emission release to or removal from the atmosphere $e^x_{r,x}$. For forests, pastures, and cropland, in general, I estimate this based on FAO (2020, Emissions - Land Use) data per region for period 2015 by dividing the stated net emissions by the documented land type area. For cropland and pastures, these data describe "carbon losses from drained histosols", for forests it is the "net carbon stock gain in the living biomass pool (aboveground and belowground)" (FAO, 2020). Where data is missing from the dataset, e.g. for pastures and cropland in Cyprus, I use a global average to estimate GHG emissions release or uptake for the land types in this region.

From the FAO datasets, there is no data available for other natural land. These comprise any mostly natural land that is not primarily grass or forest area. As such, it contains peat lands or shrubs, which I assume have net negative emissions but at a far lower rate than forests. Because of this, I estimate the net CO_2 uptake of other natural land to be 10 % of forest land in the same region. Urban is not considered for land-use emissions and valued with 0.

Land-use change emissions

Whenever the land type is changed, large parts of the overground biomass are lost, releasing the stored carbon. For simplicity, I assume that this carbon release happens instantaneous and completely. At the same time, the new land type has its own overground biomass, binding CO_2 from the atmosphere. Accounting for this, I give 20% credit of the new land types biomass, as it is young biomass that will take time to fully bind CO_2 in line with its potential. As such, I estimate CO_2 release $e^{xc}_{r,x,x'}$ ($\mathrm{t\,CO_2eq\,1000\,ha^{-1}}$) as given in (30):

$$e^{xc}_{r,x,x'} = (b_{r,x} - 0.2 \cdot b_{r,x'}) \cdot 3.67, \tag{30}$$

where $b_{r,x}$ is the carbon stock in living biomass in land type x in region r. To estimate this carbon stock for all land types, I use (FAO, 2020, Land Use) data for forest carbon stock and forest area to estimate $\mathrm{C\,ha^{-1}}$. As no data is available on the carbon stock for other land types, I use estimates from the FABLE model: relative to forest carbon stock, other natural land has 30 %, pasture 10 %, cropland 5 %, and urban areas 0 %. (Mosnier et al., 2019). $\frac{44}{16} \approx 3.67$ is the $\mathrm{CO_2 : C}$ ratio, when bound carbon is released into the atmosphere, based on their atomic weights $m^C \approx 12, m^O \approx 16$. A full table with $e^{xc}_{r,x,x'}$ values for all region r and land types x is available in the supplementary material (see Appendix).

2.3.2 Biodiversity loss

Biodiversity is affected by land type and land management system (Reidsma et al., 2006). As such, the driving force of biodiversity loss (BDL) beyond the initial period in this model is land-use change and land-management change (LMC), with 2015 setting up the initial loss due to existing land types, as shown in (31):

$$E^{BDL}_{2015,r} = \sum_{x,m} (l_{x,m} \cdot LUM_{2015,r,x,m}) \quad \forall r, \tag{31}$$

where $l_{x,m}$ is the BDL for land type x under management m, with $l_{x,m} = 1 - eq_{x,m}$, where $eq_{x,m} = [0, 1]$ is the ecosystem quality, as classified by Reidsma et al. (2006). All $b_{x,m}$ values relevant in this model are documented in table 4.
For BDL beyond 2015, I estimate the impacts from LUC and LMC as shown in (32):

$$E_{t,r}^{\text{BDL}} = \sum_{x,m,x',m'} (b_{x,m,x',m'} \cdot LC_{t,r,x,m,x',m'}) \quad \forall t, r, \tag{32}$$

$$\text{where} \quad b_{x,m,x',m'} = (b_{x,m} - b_{x',m'}) \cdot f^b_{x,m,x'm'}, \tag{33}$$

and where$f^b_{x,m,x',m'}$ is a LUC and LMC specific factor: If the old land type/management combination (x, m) is of higher ecosystem quality than the new combination (x', m'), $f^b_{x,m,x',m'} = 1$. If it's lower, leading to an increase in ecosystem quality, $f^b_{x,m,x',m'} = 0.5$, to reflect that ecosystems do not instantly recover to their full quality. In the special case of m, m' = natural, i.e. no management, (33) is not used. Instead, $b_{x,\text{nat},x',\text{nat}} = 0.5$ to reflect that by definition it is impossible to turn one natural system into another without damaging the ecosystem quality at least for some time. A complete list of $b_{x,m,x',m'}$ for all valid (x, m, x', m') combinations is available in the supplementary material (see Appendix). $LC_{t,r,x,m,x',m'}$ in (32) stores LUC and/or LMC in region r and period t for allowed combinations of x and m, as shown in (34):

$$LUM_{t,r,x,m} = LUM_{t-1,r,x,m} + \sum_{x',m'} (LC_{t,r,x',m',x,m} - LC_{t,r,x,m,x',m'}) \quad \forall t, r, x, m. \tag{34}$$

2.3.3 Deforestation, afforestation, and cropland expansion

As primary indicators for the ongoing land use and land-use change, the model assess and, depending on the scenario setup, taxes deforestation. Beyond deforestation, I also investigate changes in afforestation and cropland as additional land-use and sustainability indicators $I_{t,r}$. Using $LC_{t,r,x,m,x',m'}$, as introduced in (34), I calculate deforestation, afforestation, and cropland as shown in (35), (36), and (37), respec-

tively.

$$E_{t,r}^{\text{Def}} = \sum_{x',m'} LC_{t,r,forest,natural,x',m'} \qquad \forall t, r, x' \neq x, \tag{35}$$

$$I_{t,r}^{\text{Aff}} = \sum_{x',m'} LC_{t,r,x',m',forest,natural} \qquad \forall t, r, x' \neq x, \tag{36}$$

$$I_{t,r}^{crop} = \sum_{c,m} = C_{t,r,c,m} \qquad \forall t, r. \tag{37}$$

2.3.4 Blue and gray freshwater use

According to Mekonnen & Hoekstra (2011), rain-fed cultures often require more water in general, but most of it is green water provided through natural cycles. As this may skew the assessment of the human impact on the water sector, in this thesis, I only consider blue and gray water, as shown in (38):

$$E_{t,r}^{\text{Water}} = C_{t,r,c,m} \cdot \left(w_{r,c}^{c,b} \cdot w_{m}^{m,b} + \cdot w_{r,c}^{c,g} \cdot w_{m}^{m,g} \right) \quad \forall t, r, \tag{38}$$

where w^c and w^m are the water factors based on crop and management type for blue (b) and gray (g) water, respectively.

The average blue and gray water footprints for crop $w_{r,c}^{c,b}$ and $w_{r,c}^{c,g}$ are based on works by Mekonnen & Hoekstra (2011), where blue and gray water footprints $w_{r,p}^{\prime b/g}$ per yield of crop product p ($\text{m}^3\,\text{t}^{-1}$) are provided on a per-country basis, calculated as average 1996-2005. I estimate the average water footprint $\text{m}^3\,\text{ha}^{-1}]$, as shown in (39):

$$w_{r,c}^{c,b/g} = y_{r,c,p}^{c} \cdot y_{c,m}^{m} \cdot w_{r,p}^{\prime b/g}. \tag{39}$$

For blue water, in the EU regions, I use the blue water country averages as estimated by Mekonnen & Hoekstra (2011) as reference for irrigated farming systems. For rain-fed systems, the blue water footprint is naturally 0.

For gray water, since Mekonnen & Hoekstra (2011) estimate the gray water footprints based on nitrogen fertilizer use only, I assume this footprint to be 0 for extensive systems, as they are managed with no to very little such inputs (Reidsma et al., 2006).

Region	Countries
ASI	Afghanistan, China, India, Indonesia, Kazakhstan, Mongolia, Myanmar, Pakistan, Thailand, Uzbekistan
LAM	Argentina, Bolivia, Brazil, Chile, Colombia, Mexico, Paraguay, Peru, Venezuela
MAF	Algeria, Angola, Chad, Congo (Democratic Republic of), Egypt, Iran, Iraq, Libya, Mali, Niger, Saudi Arabia, Sudan, Yemen
NAM	Canada, United States of America
OCE	Australia, New Zealand

Table 9: Regions and their associated countries used to estimate the regional blue and gray water footprint, based on data provided by Mekonnen & Hoekstra (2011)

Organic systems may not use the same synthetic fertilizers intensive systems use, but they do use fertilizers, nonetheless. In accordance with the organic yield gap (Ponti et al., 2012), I assume both nutrient input and, following from this, gray water use to be reduced by 20%, compared to conventional systems. Since yield increases with irrigation, as determined in section 2.2, so does fertilizer application to counter the increased nutrient depletion. Because of this, I assume a 10% increase in fertilizers and, accordingly, gray water use for irrigated systems.

Where no blue or gray water footprint is available for a product, I use an EU or, if none is available, the provided global average. For the RoW regions, I use a selection of countries, shown in table 9, to average the respective crop water footprints per region and product $w'^{b/g}_{r,p}$.

2.3.5 Nitrogen and phosphorus

I calculate the nitrogen (N) and and phosphorus (P) footprints from inorganic fertilizers as shown in (40):

$$E^{N/P}_{t,r} = \sum_{c,m} \left(i^{c}_{r,i} \cdot i^{m}_{m,i} \cdot C_{t,r,c,m} \right) \quad \forall t, r, \tag{40}$$

where $i^c_{r,i}$ is the average application amount of nutrient $i = [N, P]$ in region r ($\mathrm{t\,ha^{-1}}$), and $i^m_{m,i}$ is the associated factor for management system m. Assuming that inorganic fertilizers are mostly used on cropland, I use FAO (2020, Fertilizers by Nutrient, Land Use) data on total agricultural use $\hat{i}_{r,i'}$ (t) of nitrogen (N) and phosphate (P2O5) and cropland a^c_r (1000 ha) per region r in 2015 to calculate $i^c_{r,i}$ as shown in (41).

$$i^c_{r,i} = \frac{\hat{i}_{r,i'} \cdot f^i_{i'}}{a^c_r}, \tag{41}$$

where $f^i_{i'}$ is a factor expressing the ratio of the FAO (2020) documented nutrients to their components. Specifically, $f^i_N = 1$ and, based on the atmoic weight of $P \approx 31$ and $O \approx 16$, $f^i_{P_2O_5} = \frac{62}{142} \approx 0.437$

As shown in (40), management m affects the nutrient footprint. This factor depends on the fundamental farming system and the chosen irrigation method. As with other management factors, conventional rainfed farming defines the baseline with $i^m_{c,i} = 1$. While organic systems do use fertilizers in general, by definition, they abstain from synthetic ones and, due to the yield gap, likely need to replenish fewer soil nutrients and thus apply fewer fertilizers (Mikkelsen & Hartz, 2008; Oberson & Frossard, 2005; Ponti et al., 2012). Because of this, I assume synthetic N input to be 0 in organic systems and P to be lowered in accordance with the yield gap to 80% of the baseline. Extensive systems by definition use nearly no if any inputs and abstain especially from synthetic ones (Reidsma et al., 2006). Therefore, I assume synthetic N input to be 0 in extensive systems as well and P input to be as low as 10% of the baseline.
For irrigated systems, I assume the nutrient need to increase with yield output, though not necessarily linearly. Because of this, I add 10% to all nutrient inputs. All $i^m_{m,i}$ factors are shown in table 4. A list of all $i^c_{r,i}$ values is available in the supplementary material (see Appendix).

2.3.6 Sustainability estimation

To estimate the impacts of the modeled agricultural system under different externality taxes and the interactions between different Earth system processes affected by the agricultural sector, I compare cumulative values for the modeled period 2015–2050 to their corresponding values from the tax-less base scenario and calculate the relative change R_j^E between the corresponding sustainability indicators, as shown in (42):

$$R_j^E = \frac{\sum_{t,r} \hat{I}_{t,r}^E}{\sum_{t,r,j} \hat{I}_{t,r,j}^0} \quad \forall j, \tag{42}$$

where $\hat{I}_{t,r,j} = [E_{t,r,e}, I_{t,r,a}]$, with $j = [e, a]$ and additional indicators a, afforestation and cropland, calculated in (36) and (37). Superscript E indicates the taxed externality and 0 marks the base scenario. I present and discuss the resulting R_j^E in chapter 3.

Chapter 3

Results and Discussion

I run the model as described in chapter 2 seven times. The first run, scenario 0, with $t_e = 0 \ \forall e$, defines the base which I compare all other scenario runs to. In scenario 1, I set $t_{CO_2eq} = 10,000\,\text{USD}\,\text{t}^{-1}\,\text{CO}_2\text{eq}$, in scenario 2–6, I set $t_e = 1,000,000\,\text{USD}\,/\,\text{externality unit}$ (run 2: biodiversity loss ($1000\,\text{ha}^{-1}$ carrying capacity lost), run 3: deforestation ($1000\,\text{ha}^{-1}$), run 4: fresh water use (1000m^{-3}), run 5: synthetic nitrogen (t^{-1}), run 6: phosphorus (t^{-1})). The resulting R_j^E values are shown in figures 1, 2, 3, 4, 5, and 6, respectively.

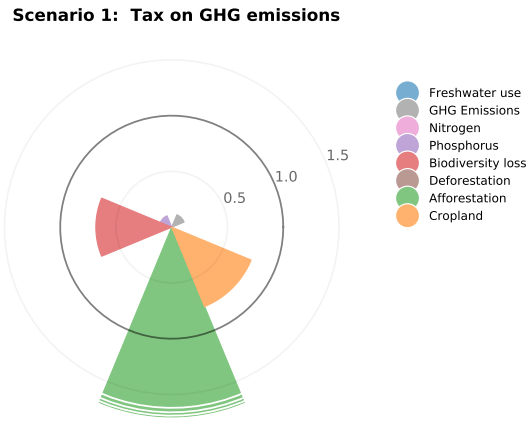

Figure 1: $R_j^{CO_2eq}$ values from scenario run 1. Values indicate relative change of sustainability indicators j in comparison to the tax-less base scenario. Interruptions in the outer cone indicate $R_j^E > 1.7$.

In Scenario 1, where I set a tax on GHG emissions, afforestation increases to as much

as 2.7 times its level in the base scenario, while all other indicators decrease alongside GHG emissions, as shown in figure 1. Most notably, deforestation, freshwater use and synthetic nitrogen application decrease to 0 or very close to it, while phosphorus drops to 11% of the base level, which seems to be the lowest level in this model possible, as even in scenario 6, where phosphorus is taxed, it does not drop lower, as shown in figure 6. Scenario 2 aside, where biodiversity loss is taxed directly, the loss level is at its lowest in scenario 1 as well, sitting at 68%, compared to the base scenario. Cropland sees a 23% drop, the smallest indicator change in this scenario but, alongside other scenarios, the largest cropland change modeled.

Due to the associated tax, scenario 2, shown in figure 2, brings biodiversity loss to the lowest level between the six scenarios, at 26% of the base scenario. Forests see no change, as there is neither deforestation nor afforestation in this scenario. As in scenario 1, 23% of the base scenario cropland is freed up. At 39%, GHG emissions go to their lowest level aside from scenario 1. Nitrogen, phosphorus, and fresh water levels, while not at their lowest possible point when compared to other scenarios, all drop very low relative to the baseline, at 5, 16, and 18 %, respectively.

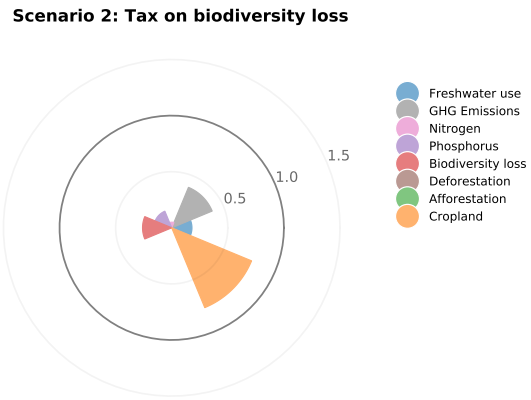

Figure 2: R_j^{BDL} values from scenario run 2. Values indicate relative change of sustainability indicators j in comparison to the tax-less base scenario.

Taxing deforestation in scenario 3, shown in figure 3, brings this indicator to 0, while most others either drop only little or increase in turn. Cropland shrinks by 7%, along-

side biodiversity loss, which drops by 10%, and GHG emissions, dropping by 13%. On the other hand, the water, nitrogen and phosphorus footprints increase beyond base levels to 102, 117, and 110%, respectively. And, while deforestation sinks, so does afforestation – by 75% compared to the base scenario. Only scenario 2 goes lower.

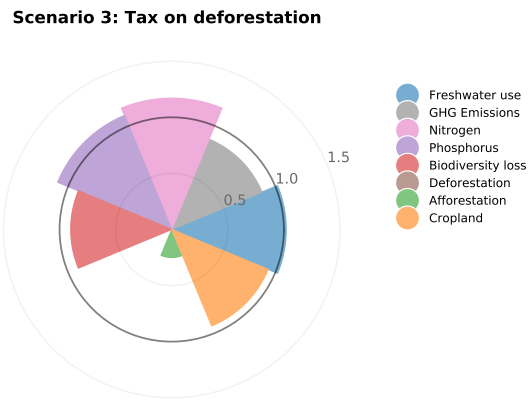

Figure 3: R_j^{Defor} values from scenario run 3. Values indicate relative change of sustainability indicators j in comparison to the tax-less base scenario.

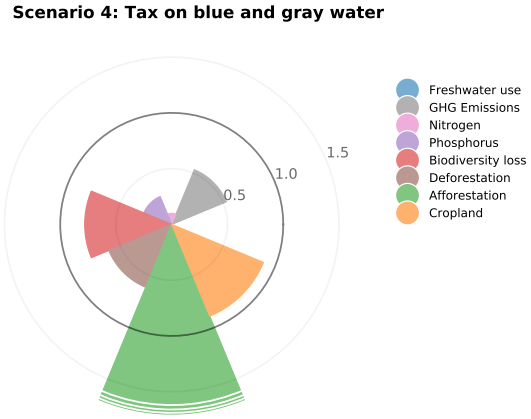

Figure 4: R_j^{Water} values from scenario run 4. Values indicate relative change of sustainability indicators j in comparison to the tax-less base scenario. Interruptions in the outer cone indicate $R^{\hat{I},E} > 1.7$.

Scenario 4 taxes blue and gray water use and naturally forces them to their lowest possible level, close to 0. At the same time, all other indicators shrink, with he exception of afforestation which reaches its highest point, scenario 1 aside, at 179% of the

base level. At the same time, cropland drops by 11%, deforestation by 39%. GHG emissions are cut by nearly half, shrinking to 53%. Biodiversity loss goes down to 70% of the baseline value. Phosphorus and nitrogen drop even further to 27 and 10% of their respective base levels.

Figure 5 shows the taxation scenario for synthetic nitrogen. While this fertilizer input drops to 0, few indicators move with it. GHG emissions drop by 14%, one of the smallest drops in all scenarios. Water use also declines but only by 16%. Cropland and biodiversity loss are nearly unchanged at 100 and 99% of the baseline levels. At the same time, phosphorus input increases by 5% and deforestation goes up by 30%. However, this is partly balanced out by an 20% increase in afforestation.

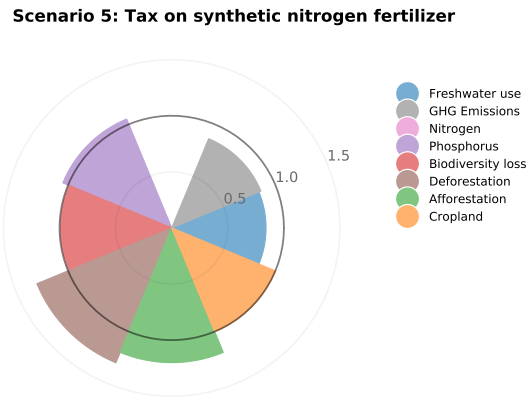

Figure 5: R_j^{N} values from scenario run 5. Values indicate relative change of sustainability indicators j in comparison to the tax-less base scenario. Values indicate relative change of sustainability indicators in comparison to the tax-less base scenario.

Lastly, figure 6 shows the tax scenario on phosphorus pollution, reducing phosphorus application to 11% of its base value. Nitrogen and water use shrink even further and go down to 0. GHG emissions and biodiversity loss also shrink drastically alongside phosphorus, down to 52 and 70%. While cropland is reduced by 23% and afforestation increases by 30%, deforestation also increases by 24%, reducing the additional forest's positive climate impact.

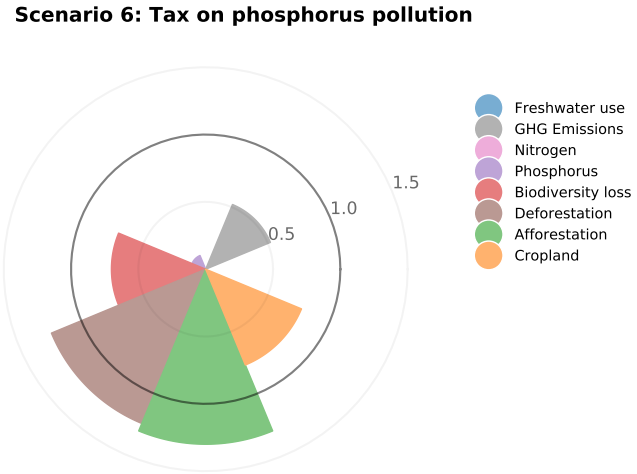

Figure 6: R_j^{P} values from scenario run 6. Values indicate relative change of sustainability indicators j in comparison to the tax-less base scenario. Values indicate relative change of sustainability indicators in comparison to the tax-less base scenario.

What seems obvious from figure 5, is that primarily reducing synthetic nitrogen has little co-benefits in this model. On the other hand, the nitrogen indicator profits from most of the other taxes. As shown in figure 7, that is because many tax scenarios shift crop production mostly or completely towards extensive farming where application of synthetic nitrogen is forbidden, with the exception of deforestation which does not profit from the reduced area efficiency. The nitrogen tax moves crop production to an otherwise rare management system in the run scenarios, irrigated organic farming, which provides the second highest yields while prohibiting nitrogen application.

Similarly, deforestation has few obvious strong interactions with other indicators, as visible in figure 3. Only afforestation shows changes similar in size to the 100% reduction of deforestation. This makes intuitively sense, as the model balances out the inavailability of land that was available for cropland or pasture expansion in the base scenario by keeping other areas from being afforested. These are likely less efficient than the ones deforested in the base scenario but necessary for profit maximization. The lower efficiency of these now not-afforested areas also shows in the crop-management distribution in figure 7.

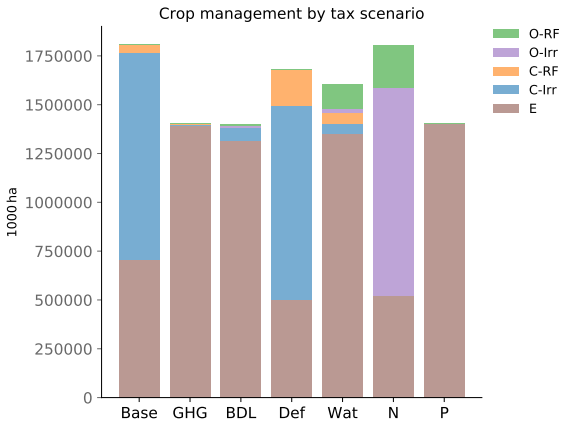

Figure 7: 2015–2050 annual average area (1000 ha) of cropland managed in the different available management systems by tax scenario. Management systems are conventional (C), organic (O), and extensive (E), either rainfed (RF) or irrigated (Irr). Scenarios are the base scenario (run 0), and taxation of GHG (run 1: GHG), biodiversity loss (run 2: BDL), deforestation (run 3: Def) water use (run 4: Wat), synthetic nitrogen (run 5: N), and phosphorus (run 6: P).

While cropland is overall reduced, conventional farming increases relatively, especially C-RF, whose absolute area grows by more than 300%, leading to a 380% growth of its relative share of cropland. This may also be the reason why the synergies with climate protection and biodiversity integrity are surprisingly weak. On one hand, limiting deforestation directly reduces GHG emissions and biodiversity loss from LUC and habitat destruction, both of which are penalized stronger in this model than the same level of afforestation would be rewarded, making it more efficient in these regards to not remove forest instead of replanting what has been removed. On the other hand, shifting to higher efficiency systems is associated with higher emissions over time and lower ecosystem quality on these areas, as shown in table 4.

While nitrogen can be strongly reduced by shifting from one high-yield management system to another slightly less efficient one, the second investigated nutrient, phosphorus, can not. It needs a more vast shift. One difference between the two is this model's focus on synthetic nitrogen from the atmosphere (in contrast to nitrogen pollution from other sources, such as manure), which is completely prohibited for some management systems, while phosphorus pollution is an issue that I assume to affect

all systems, albeit to different degrees. Because of this, the phosphorus footprint can not be reduced to 0 and any reduction greatly affects yield efficiency. Since the tax affects all management systems, it incentivizes minimizing cropland as much as possible and maximizing its extensive management share, as visible in figure 7. This management change also explains the well expressed synergies. In this model, crop production is the only source of freshwater use, which is reduced to 0 on extensively managed areas, as is nitrogen application.

Considering the relatively low yield efficiency of extensive farming in this model, it is no surprise that the consumption patters change significantly in this scenario as well, as visible in figure 8 and 9. Both crop and livestock product consumption is limited to an efficient minimum, while the model specializes on high caloric but low value oil products, specifically rapeseed oil, and milk, which refines feed crops and increases their value.

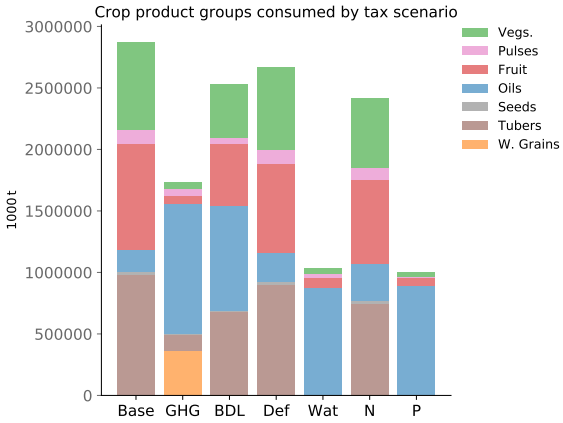

Figure 8: 2015–2050 annual average amount (1000 t) of direct human consumption of crop primary and secondary products. Product groups are whole grains (wheat, sorghum, rice, millet, barley, maize), tubers and starchy roots (potatoes, cassava), seeds (sunflower, rapeseed), oils (sunflower, rapeseed, olive, soy, palm), fruit (apples, bananas, oranges), pulses (beans, chickpeas, soybeans), and vegetables (tomatoes, onions, olives). Scenarios are the base scenario (run 0: base), and taxation of GHG (run 1: GHG), biodiversity loss (run 2: BDL), deforestation (run 3: Def) water use (run 4: Wat), synthetic nitrogen (run 5: N), and phosphorus (run 6: P).

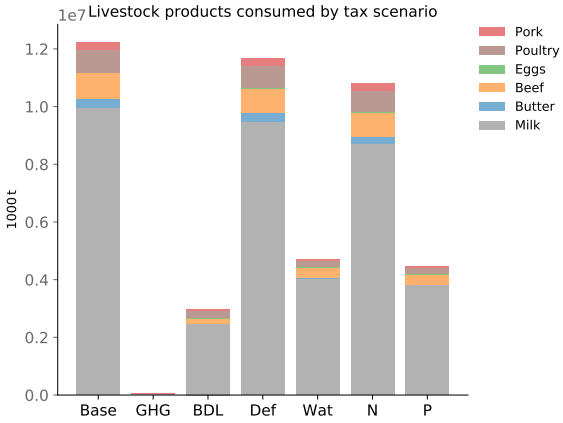

Figure 9: 2015–2050 annual average amount (1000 t) of direct human consumption of livestock primary and secondary products. Milk comprises both milk and skimmed milk. Scenarios are the base scenario (run 0: base), and taxation of GHG (run 1: GHG), biodiversity loss (run 2: BDL), deforestation (run 3: Def) water use (run 4: Wat), synthetic nitrogen (run 5: N), and phosphorus (run 6: P).

High deforestation combined with high afforestation possibly stems from the need to minimize cropland to reduce the phosphorus impact while also specializing on most efficient areas. So, while areas with high rapeseed yield are deforested, others with lower yield are afforested to reduce the cropland impact. This back and forth reduces the otherwise positive impact the cropland reduction has on GHG emissions and biodiversity loss reduction. Even with these limitations, in the model as it is currently set-up, there are clearly positive interconnections between P, GHG, and BDL reductions.

Taxing blue and gray water use, shown in figure 4, results in similar behavior to the phosphorus scenario, with a strong shift towards extensive crop management, roughly doubling extensively managed cropland and limiting crop production nearly completely to this very water-efficient system. Cropland and nitrogen reduction are less pronounced but so is deforestation, while afforestation is even higher. As did water from the phosphorus tax, now the phosphorus indicator profits from the water-tax induced management shift. Accordingly, consumption also shifts to the same high-oil, high-milk diet, shown in figures 8 and 9.

The tax on GHG emissions has the opposite effect. Here, consumption moves nearly completely away from livestock products. This makes sense, as these products have multiple GHG impacts – through the necessary feed as well as through direct livestock emissions. Because of this, it is not surprising that faced with a steep price on CO_2eq the model finds more efficient pathways without livestock consumption. This apparent strong leverage is likely directly related to a somewhat radical diet shift between the base scenario and scenario 1. As they are no longer most efficient as feed, whole grain products are shifted to human consumption. This way cropland can shrink despite the lower yield efficiency of the nearly exclusively extensive crop management. As long as enough space is available without the need for emission-intensive LUC, shifting to extensive management seems sensible, using parameters as assumed for this thesis. While yields drop by 80%, emissions from two sources vanish nearly completely. Further emissions shrink and grow with yield, making extensive farming, in this model, competitive in this regard as well. Furthermore, as with all scenarios that shift to extensive management, water, phosphorus, and nitrogen impacts are reduced here as well. Additionally, biodiversity profits from mostly conventionally managed pastures being turned into forests, as can be assumed from figures 10 and 11, which is an ecosystem quality gain despite the reduced credit. The tax motivated blockage of deforestation is an additional plus for biodiversity protection. This behavior may of course change with a more complex model, reflecting the complex properties of different land types and regions, or the labor-intensive processes and crop interactions especially important in organic and extensive farming.

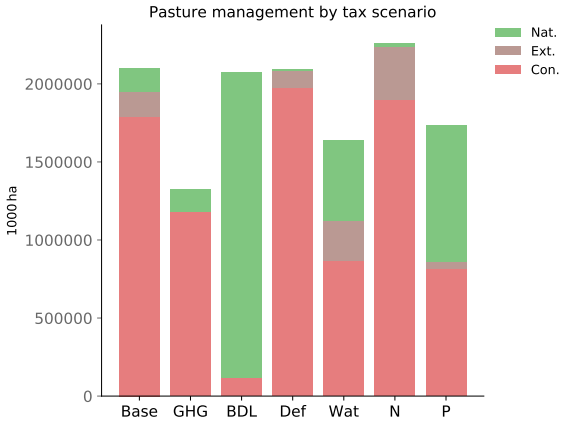

Figure 10: 2015–2050 annual average area (1000 ha) of pasture under extensive (Ext.) or conventional (Con.) management or without management (Nat.). Scenarios are the base scenario (run 0: base), and taxation of GHG (run 1: GHG), biodiversity loss (run 2: BDL), deforestation (run 3: Def) water use (run 4: Wat), synthetic nitrogen (run 5: N), and phosphorus (run 6: P).

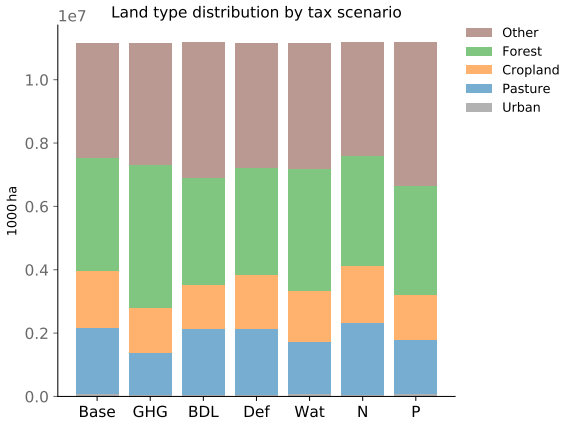

Figure 11: 2015–2050 annual average area (1000 ha) of global cropland, forest, pasture, urban, and other natural land. Scenarios are the base scenario (run 0: base), and taxation of GHG (run 1: GHG), biodiversity loss (run 2: BDL), deforestation (run 3: Def) water use (run 4: Wat), synthetic nitrogen (run 5: N), and phosphorus (run 6: P).

Tax	Synergy	Conflict
GHG	Afforestation (198%), water (114%), N (113%), deforestation (113%), P (101%), BDL (36%), cropland (26%)	-
BDL	Deforestation (136%), N (129%), P (101%), water (111%), GHG (83%), cropland (31%)	Afforestation (134%)
Def	GHG (13%), BDL (10%), cropland (7%)	Afforestation (75%), N(17%), P (10%), water (2%)
Water	N (90%), afforestation (79%), P (73%), GHG (47%), deforestation (39%), BDL (22%) cropland (11%)	-
N	Afforestation (20%), water (16%), GHG (14%), BDL (1%)	Deforestation (30%), P (5%)
P	N (112%), water (112%), GHG (54%), BDL (34%), afforestation (34%), cropland (25%)	Deforestation (26%)

Table 10: Synergies and conflicts between planetary impacts expressed as change relative to the change of taxed externality. Synergies occur when the taxed externality and a sustainability indicator grow or shrink together, where percentages express the relative growth. For afforestation, it is considered a synergy if it grows while the taxed externality shrinks and vice-versa.

The overall most pronounced changes are visible in figure 2 for the tax on biodiversity loss. Cropland aside, all indicators drop below 50%, five of them even below 20% of baseline levels. Similar to runs 1, 4, and 6, this is associated with a strong increase in extensive crop management, shown in figure 7. Additionally, pasture management sees large changes as well, with most of it turning to natural management, increasing its ecosystem quality but reducing its livestock carrying capacity.

Co-evolution of GHG emissions and biodiversity loss could even be more pronounced if the model had been solved in a way that shifts the increase in other natural land,

shown in figre (11), to forests instead. In this model, this should be easily possible, as both land types have the same ecosystem quality and would bring with it the forest's assumed higher CO_2 sequestration rate. A slight shift in parameter choices could possibly change this and increase the BDL-GHG synergy without affecting the others.

All synergies and conflicts between the investigated planetary impacts are listed in table 10, where the percentage is the relative size of the change of each indicator to the change in the taxed externality. Afforestation, as one indicator for land-system change, shows both the strongest synergy (198% relative to GHG in scenario 1) and the strongest conflict (134% relative to BDL in scenario 2). While the additional indicators for land-system change are mixed between synergies and conflicts, the main indicator, cropland, shows consistent synergies in a range of 20–30% with all externality reductions but nitrogen. Most prominent are the interactions between GHG, BDL, water, and P, which are consistently on high levels, with cropland and N also benefiting, despite the limited synergies the N scenario shows.

These results are of course highly dependent on the complexity of the model and the parameter choices. For example, the consumption mix of mostly milk and oil in several scenarios highlights a current weakness the model has. While it aims to reflect real production mixes, consumption can easily become highly specialized, which should be addressed by adding a consumption mix corridor or demand functions.
Also very noticeable is the apparent versatility of extensive crop management as a solution for any kind of planetary impact from land use. While this could be true in principle, it is likely that the parameter estimates for extensive farming are very optimistic, due to the lack of data on large scale extensive operations, and not enough constraints were put in place to reflect special requirements, such as crop rotation or multiple cropping.

As a first step towards a larger model for estimating interconnections between planetary impacts, the framework created in this thesis is limited by several such simplifica-

tions, both in data aggregation and in the model structure: Land type categorization is very broad and, within the defined LUC corridor, the model allows to change from any to any type without regard for important real world limitations, such as climatic or soil suitability. Furthermore, the RoW regions are, as was the intention, very large, including very different climate zones and economic realities. Sorting them into sub-regions, while also including parts of the world so far ignored in the model, may make the results more reliable.

In the production estimates, water should be added as resource, likely significantly limiting production in general and specific management practices in some parts of the world. At the same time, green water could be investigated alongside blue and gray, both as a single aspect and in a combined total footprint. Forests are currently not considered as production areas with different management options and consumable output. Similarly, bio-fuel production and consumption is currently ignored. For livestock production, emission estimates as well as the global feed mix and cost need to be revisited.

Chapter 4

Conclusion

In this thesis, I set out to estimate the interconnections between planetary impacts, as described by Rockström et al. (2009a), associated with the land-use sector. To do so, I created a new agricultural-sector model, estimating greenhouse gas emissions, biodiversity loss, biogeochemical flows of nitrogen and phosphorus, blue and gray freshwater consumption, and land-system change while ensuring that SDG 2, zero hunger, is reached. Taxing one of the planetary impacts, I compared its change with the changes in the others and associated sustainability indicators to investigate how large synergies and conflicts between impact reductions are.

I have found, in the framework of this model, that there are strong synergies between reductions of greenhouse gas emissions, biodiversity loss, water consumption, and phosphorus pollution, where reducing any one of these will reduce the others by at least 20%, often 30% or more, and up to over 100% relative to the taxed externality's change, as shown in table 10. Additionally, reducing any of these four also has positive impacts on nitrogen application and cropland reduction, although additional indicators for land-system change, i.e. deforestation and afforestation, are not linked as clearly. At the core of many of these interactions is likely a large scale shift in crop management systems between the base scenario and the investigated ones, where all of these connected ones specialize to large degrees in extensive farming on a reduced cropland area.

On the other hand, primarily reducing deforestation shows weak synergies with some

indicators and weak conflicts with others. This is similarly true for nitrogen application, despite this impact indicator profiting more strongly from reductions in others.

Due to the many simplifications in this model, these results can only be an indicator for possible interactions between planetary impacts from the land-use sector and potential sustainable pathways towards reducing these impacts. Nonetheless, this thesis contributes to our understanding of the issue while also highlighting topics and questions for future research, regarding e.g. the importance of extensive farming.

References

Alkire, S., Conceição, P., Calderón, C., Dirksen, J., Evans, M., Gonzales, R., ... Suppa, N. (2020). *Global multidimensional poverty index 2020.* Retrieved December 3, 2020, from http://hdr.undp.org/sites/default/files/2020_mpi_report_en.pdf

Campbell, B., Beare, D., Bennett, E., Hall-Spencer, J., Ingram, J., Jaramillo, F., ... Shindell, D. (2017). Agriculture production as a major driver of the earth system exceeding planetary boundaries. , *22*(4). Retrieved October 20, 2020, from https://www.ecologyandsociety.org/vol22/iss4/art8/#introduction32 (Publisher: The Resilience Alliance) doi: 10.5751/ES-09595-220408

Ceballos, G., Ehrlich, P. R., Barnosky, A. D., García, A., Pringle, R. M., & Palmer, T. M. (2015). Accelerated modern human–induced species losses: Entering the sixth mass extinction. , *1*(5), e1400253. Retrieved from https://advances.sciencemag.org/content/1/5/e1400253 (Publisher: American Association for the Advancement of Science Section: Research Article) doi: 10.1126/sciadv.1400253

Chilonda, P., & Otte, J. (2006). Indicators to monitor trends in livestock production at national, regional and international levels. , *18*(8). Retrieved November 23, 2020, from https://doi.org/10.3390/su7010947

Crutzen, P. J. (2002). Geology of mankind. , *415*(6867), 23–23. Retrieved October 20, 2020, from https://www.nature.com/articles/415023a doi: 10.1038/415023a

EUROSTAT. (2020a). *Freight transport statistics - modal split.* Retrieved November 1, 2020, from https://ec.europa.eu/eurostat/statistics-explained/index.php/Freight_transport_statistics_-_modal_split

EUROSTAT. (2020b). *International trade in goods by mode of transport.* Retrieved November 1, 2020, from https://ec.europa.eu/eurostat/statistics-explained/index.php/International_trade_in_goods_by_mode_of_transport#Trade_by_mode_of_transport_in_value_and_quantity

EUROSTAT. (2020c). *Intra-eu trade in goods - main features.* Retrieved November 1, 2020, from https://ec.europa.eu/eurostat/statistics-explained/index.php?oldid=452727#Intra-EU_trade_in_goods_compared_with_extra-EU_trade_in_goods

FAO. (1997). *Irrigation technology transfer in support of food security* (No. 14). Retrieved October 16, 2020, from http://www.fao.org/3/W7314E/w7314e0h.htm

FAO. (2020). *FAOSTAT.* Retrieved October 15, 2020, from http://www.fao.org/faostat/en/ ([Database])

Georg, S. (2020). *Distance calculator.* Retrieved October 11, 2020, from https://www.distance.to/ ([Database])

Hasegawa, T., Havlík, P., Frank, S., Palazzo, A., & Valin, H. (2019). Tackling food consumption inequality to fight hunger without pressuring the environment. , *2*(9), 826–833. Retrieved from https://www.nature.com/articles/s41893-019-0371-6 (Number: 9 Publisher: Nature Publishing Group) doi: 10.1038/s41893-019-0371-6

Hoegh-Guldberg, O., Jacob, D., Taylor, M., Bindi, M., Brown, S., Camilloni, I., ... Zhou, G. (2018). *Impacts of 1.5^{o}c global warming on natural and human systems.* Retrieved October 20, 2020, from https://www.ipcc.ch/site/assets/uploads/sites/2/2019/02/SR15_Chapter3_Low_Res.pdf (Masson-Delmotte, V., P. Zhai, H.-O. Pörtner, D. Roberts, J. Skea, P.R. Shukla, A. Pirani, W. Moufouma-Okia, C. Péan, R. Pidcock, S. Connors, J.B.R. Matthews, Y. Chen, X. Zhou, M.I. Gomis, E. Lonnoy, T. Maycock, M. Tignor, and T. Waterfield (eds.))

Hug, L., Alexander, M., You, D., & Alkema, L. (2019). National, regional, and global levels and trends in neonatal mortality between 1990 and 2017, with scenario-based projections to 2030: a systematic analysis. , *7*(6), e710–e720. Retrieved from https://www.thelancet.com/journals/langlo/article/PIIS2214-109X(19)30163-9/abstract (Publisher: Elsevier) doi: 10.1016/S2214-109X(19)30163-9

IPBES. (2019). *Global assessment report on biodiversity and ecosystem services of the intergovernmental science-policy platform on biodiversity and ecosystem services.* Retrieved October 20, 2020, from https://ipbes.net/global-assessment (Brondizio, E. S. and Settele, J. and Díaz, S. and Ngo,H. T. (eds.))

IPCC. (2014). *Climate change 2014: Synthesis report. contribution of working groups i, ii and iii to the fifth assessment report of the intergovernmental panel on climate change.* Retrieved from https://www.ipcc.ch/site/assets/uploads/2018/02/SYR_AR5_FINAL_full.pdf (Core Writing Team, R.K. Pachauri and L.A. Meyer (eds.))

KC, S., & Lutz, W. (2017). The human core of the shared socioeconomic pathways: Population scenarios by age, sex and level of education for all countries to 2100. *Global Environmental Change*, *42*, 181–192. doi: 10.1016/j.gloenvcha.2014.06.004

Lambert, J. (1988). *Village milk processing* (No. 69). Retrieved October 23, 2020, from http://www.fao.org/3/T0045E/T0045E00.htm

Mekonnen, M. M., & Hoekstra, A. Y. (2011). The green, blue and grey water footprint of crops and derived crop products. , *15*(5), 1577–1600. Retrieved from https://hess.copernicus.org/articles/15/1577/2011/ doi: 10.5194/hess-15-1577-2011

Mikkelsen, R., & Hartz, T. (2008). *Nitrogen sources for organic crop production* (Vol. 92). Retrieved November 11, 2020, from http://www.ipni.net/publication/bettercrops.nsf/0/F5447D476D6E58458525798000708D98/$FILE/Better%20Crops%202008-4%20p16.pdf

Mosnier, A., Penescu, L., Thomson, M., & Perez-Guzman, K. (2019). *Fable calculator documentation.* Retrieved November 20, 2020, from https://faa0182d-ea6b-4a7b-8da9-4789e4379e59.filesusr.com/ugd/89a4db_970e78be1faa4eb6a6ba62c8ef0550c5.pdf?index=true

Oberson, A., & Frossard, E. (2005). Phosphorus management for organic agriculture. In J. Sims & A. Sharpley (Eds.), *Phosphorus: Agriculture and the environment* (Vol. 46). doi: https://doi.org/10.2134/agronmonogr46.c24

O'Neill, D. W., Fanning, A. L., Lamb, W. F., & Steinberger, J. K. (2018). A good life for all within planetary boundaries. , *1*(2), 88–95. Retrieved October 20, 2020, from https://www.nature.com/articles/s41893-018-0021-4 (Number: 2 Publisher: Nature Publishing Group) doi: 10.1038/s41893-018-0021-4

Papargyropoulou, E., Lozano, R., K. Steinberger, J., Wright, N., & bin Ujang, Z. (2014). The food waste hierarchy as a framework for the management of food surplus and food waste. *Journal of Cleaner Production*, *76*, 106 - 115. Retrieved from http://www.sciencedirect.com/science/article/pii/S0959652614003680 doi: https://doi.org/10.1016/j.jclepro.2014.04.020

Ponti, T. d., Rijk, B., & Ittersum, M. K. v. (2012). The crop yield gap between organic and conventional agriculture. , *108*, 1 – 9. Retrieved from http://www.sciencedirect.com/science/article/pii/S0308521X1100182X doi: https://doi.org/10.1016/j.agsy.2011.12.004

Randers, J., Rockström, J., Stoknes, P.-E., Goluke, U., Collste, D., Cornell, S. E., & Donges, J. (2019). Achieving the 17 sustainable development goals within 9 planetary boundaries. , *2*. Retrieved October 20, 2020, from https://www.cambridge.org/core/journals/global-sustainability/article/achieving-the-17-sustainable-development-goals-within-9-planetary-boundaries/5934F82F471B751168A0B2AE59AD0319 (Publisher: Cambridge University Press) doi: 10.1017/sus.2019.22

Reidsma, P., Tekelenburg, T., Berg, M. v. d., & Alkemade, R. (2006). Impacts of land-use change on biodiversity: An assessment of agricultural biodiversity in the european union. , *114*(1), 86 – 102. Retrieved from http://www.sciencedirect.com/science/article/pii/S0167880905005360 doi: https://doi.org/10.1016/j.agee.2005.11.026

Riahi, K., van Vuuren, D. P., Kriegler, E., Edmonds, J., O'Neill, B. C., Fujimori, S., ... Tavoni, M. (2017, jan). The shared socioeconomic pathways and their energy, land use, and greenhouse gas emissions implications: An overview. *Global Environmental Change*, *42*, 153–168. doi: 10.1016/j.gloenvcha.2016.05.009

Rockström, J., Steffen, W., Noone, K., Persson, A., Chapin, F. S., Lambin, E. F., ... Foley, J. A. (2009b). A safe operating space for humanity. , *461*(7263), 472–475. Retrieved from https://www.nature.com/articles/461472a doi: 10.1038/461472a

Rockström, J., Steffen, W., Noone, K., Persson, A., Chapin, F. S. I., Lambin, E., ... Foley, J. (2009a). Planetary boundaries: Exploring the safe operating space for humanity. , *14*(2). Retrieved from https://www.ecologyandsociety.org/vol14/iss2/art32/ doi: 10.5751/ES-03180-140232

Sgroi, F., Candela, M., Trapani, A., Foderà, M., Squatrito, R., Testa, R., & Tudisca, S. (2015). Economic and financial comparison between organic and conventional farming in sicilian lemon orchards. , *7*(1), 947–961. doi: https://doi.org/10.3390/su7010947

Steffen, W., Richardson, K., Rockström, J., Cornell, S. E., Fetzer, I., Bennett, E. M., ... Sörlin, S. (2015). Planetary boundaries: Guiding human development on a changing planet. , *347*(6223). Retrieved October 20, 2020, from https://science.sciencemag.org/content/347/6223/1259855 (Publisher: American Association for the Advancement of Science Section: Research Article) doi: 10.1126/science.1259855

Tuomisto, H. L., Hodge, I. D., Riordan, P., & Macdonald, D. W. (2012). Does organic farming reduce environmental impacts? – a meta-analysis of european research. , *112*, 309 – 320. Retrieved from http://www.sciencedirect.com/science/article/pii/S0301479712004264 doi: https://doi.org/10.1016/j.jenvman.2012.08.018

UN. (2017). *Work of the statistical commission pertaining to the 2030 agenda for sustainable development.* Retrieved December 3, 2020, from https://undocs.org/pdf?symbol=en/A/RES/71/313

UNDP. (2018). *Human development indicators and indices: 2018 statistical update.* Retrieved December 3, 2020, from http://hdr.undp.org/sites/default/files/2018_human_development_statistical_update.pdf

UNEP. (2018). *The adaptation gap report 2018.* Retrieved October 20, 2020, from https://www.unenvironment.org/resources/adaptation-gap-report

United Nations Conference on Trade and Development. (2017). *Review of maritime transport 2017.* Retrieved November 17, 2020, from https://unctad.org/system/files/official-document/rmt2017_en.pdf

U.S. Department of Agriculture. (2020). *What's in the foods you eat search tool.* Retrieved October 21, 2020, from https://www.ars.usda.gov/northeast-area/beltsville-md-bhnrc/beltsville-human-nutrition-research-center/food-surveys-research-group/docs/whats-in-the-foods-you-eat-search-tool/ ([Database])

U.S. Department of Health and Human Services, & U.S. Department of Agriculture. (2015). *2015-2020 dietary guidelines for americans.* Retrieved from http://health.gov/dietaryguidelines/2015/guidelines (8th Edition)

Weber, C. L., & Matthews, H. S. (2008). Food-miles and the relative climate impacts of food choices in the united states. , *42*(10), 3508–3513. doi: 10.1021/es702969f

Appendix

The model code and supplementary material is available online at

`https://github.com/jansteinhauser/masc`.

I	Model regions (excluding EU-28 countries) in FAOSTAT and SSP database
IIa	Readjusted age groups for MDER calculation based on SSP population projection
IIb	MDER scaled to annual values per region and period
III	Crop parameters
IV	Livestock parameters
V	2010 land cover data
VI	Process parameters
VII	Region-region trade distances
VIII	Emission factors for LUC-LUM combinations
IX	Biodiversity loss factors for LUC-LUM combinations
X	Nitrogen and phosphorus input ($\mathrm{t\,ha^{-1}}$) by region and nutrient

Acknowledgments

Far too many people have been part of the journey leading to this thesis to name them all. Nonetheless, I am grateful to every single one of you and appreciate how all of you have shaped and influenced me, helped with little insights and recommendations or just the right link at just the right time – or simply through an act of kindness in times that are more trying than many of us would like to admit.

That being said, there are those I can and need to name for their special importance in this work. Foremost, of course, I thank my supervisor, Prof. Dr. Uwe Schneider, for the many opportunities he has provided me with and the trust he has put in me since I first joined his research unit. I appreciate all the things I've learned from and through him as much as his support, encouragement, and flexibility over the course of these recent month. I also thank Dr. Livia Rasche, my second supervisor, for her quick responses and insights that, if they haven't found their way into this work, surely will influence future research.

I am glad to count among my friends smart and caring people, like Paridhi and Georg, who not only encouraged me and provided valuable feedback but who also were important anchors for my sanity during long writing sessions. And I am still thankful to Auriane, Mark, and the entire lab group PG409 from my physics days for their support whenever I struggled with differential equations. While it's been years at this point, I'm not sure I could hand this thesis in now without them. However, among all my friends, the one who deserves most praise is without a doubt Konrad, who has taken hours and hours out of his busy days, sometimes on very short notice,

to dive deep into my equations and make sure everything is where it belongs, and whose critical feedback I always take to heart as it has always made my work better.

And, of course, Doris, who has shown me more love, support, and patience during the work on this thesis than I could ever have asked for, who has been my consistent (and sometimes rightly complaining) sparring partner for new ideas as well as celebrations after frustrating debugging phases. I couldn't have met you at a better time.

Last but not least, I thank my family, especially my parents Johannes and Elizabeth and my late grandmother Brigitte for their unwavering support and encouragement. They've shared so many great experiences with me, influenced me in so many ways, and enabled me to do so many of the things I have done that I will never be able to repay them. The little thing I can do is dedicate this work to my grandmother who sadly passed not long ago and who will be dearly missed.

To all of you from the bottom of my heart: Thank you.